Identifying G protein-coupled receptor dimers from crystal packings

Authors

Ronald E. Stenkamp[a]*

[a]Depts. of Biological Structure and Biochemistry, Biomolecular Structure Center, University of Washington, Box 357140, Seattle, Washington, 98112, United States

Correspondence email: stenkamp@u.washington.edu

Dimers of G protein-coupled receptors are believed to be important for signaling with their associated G proteins. Low resolution electron microscopy shows rhodopsin dimers in native retinal membranes, and CXCR4 dimers are found in several different crystal structures. Evidence for dimers of other GPCRs is more indirect. An alternative to computational modeling studies is to search for parallel dimers in the packing environments of the reported crystal structures of GPCRs. Two major structural types of GPCR dimers exist (as predicted by others), but there is considerable structural variation within each cluster. The different structural variants described here might reflect different functional properties and should provide a range of model structures for computational and experimental examination.

1. Introduction

Do G protein-coupled receptor (GPCR) dimers exist, and if they do, what do they look like? These are long-standing questions important for understanding GPCR function. Images of ordered arrays of rhodopsin in native membranes (Fotiadis *et al.*, 2003, Liang *et al.*, 2003, Filipek *et al.*, 2004) are consistent with dimers and higher oligomers, and electron microscopic studies of transducin/rhodopsin complexes further indicate that rhodopsin dimers exist and are physiologically functional (Jastrzebska *et al.*, 2011, Jastrzebska *et al.*, 2013). Other GPCRs are also believed to form

dimers (Palczewski & Orban, 2013, Ferre *et al.*, 2014, Kasai & Kusumi, 2014, Vischer *et al.*, 2015, Gahbauer & Böckmann, 2016, Farran, 2017, Tian *et al.*, 2017).

Crystal structure determinations of GPCRs have shown their basic protein folding topology of seven transmembrane helices (TM1 through TM7), and in some GPCRs, an eighth helix (H8) oriented parallel to the membrane surface. Analysis of crystal packing interactions (Katritch *et al.*, 2013) led to the suggestion of two possible interfaces involved in dimer formation. . One such interface involves transmembrane helices 1 (TM1) and TM2 as well as helix H8. Other interfaces of interest make use of TM3, TM4, TM5 and TM6. Most of these interfaces are small in area, with no amino acid residues sufficiently buried to be considered "core" residues. Computational analysis of these interfaces (Duarte *et al.*, 2013) suggests that most of them do not result in physiologically relevant dimers. More recently, Baltoumas, *et al.* (Baltoumas *et al.*, 2016) used molecular dynamics calculations to investigate the stability and dynamics of potential dimers extracted from crystal structures along with dimers modelled de novo. Their results are consistent with these two major candidates for dimer interfaces.

Over 200 crystal structures of GPCRs have been deposited in the Protein Data Bank (PDB) (Berman *et al.*, 2000) since the structure of rhodopsin was solved in 2000 (Palczewski *et al.*, 2000). This project investigates whether there are examples of GPCR-GPCR interactions in crystals that can be models of functional GPCR dimers. These might provide starting points for computational modelling or other experimental approaches probing for physiological dimers of biomedical interest. Reported here are the results of looking for GPCR dimers in the crystal structures.

2. Materials and Methods

A list of GPCR crystal structures was assembled by collating the results of keyword searches at the PDB website and lists found in review articles (Okada, 2012, Piscitelli *et al.*, 2015) and in GPCR database websites (GPCRdb, http://gpcrdb.org/ (Isberg *et al.*, 2016); Membrane Proteins of Known 3D Structure, http://blanco.biomol.uci.edu/mpstruc/). Table 1 lists the 215 entries in the initial set of crystal structures and the 121 crystal forms containing GPCR transmembrane domains.

The deposited structural models include many non-protein moieties such as crystallization agents, ligands, agonists, antagonists, post-translational modifications, and peptide or protein inhibitors. Non-covalently bound groups were removed from the structural models since the focus of this study is on protein-protein interactions that might mimic subunit interactions in dimers.

Crystal packing environments for the GPCR molecules were generated and analysed using a mix of programs in the CCP4 program suite (Winn *et al.*, 2011) and locally written programs. Space group symmetry operations were applied using pdbset to generate the molecules surrounding each GPCR in their crystalline lattice. Molecules were considered part of the packing environment for each crystallographically unique GPCR if they had atoms within 4.0 Å of atoms in the central (or base) molecule. The CCP4 superpose program (Krissinel & Henrick, 2004) was used to align the environments on the basis of the central GPCRs. The packing environments were further dissected to generate pairs of interacting GPCRs. For each pair, buried solvent accessible surfaces (bSAS) were calculated using areaimol (Lee & Richards, 1971, Saff & Kuijlaars, 1997).

XtalView (McRee, 1999) and Coot (Emsley *et al.*, 2010) were used for molecular visualization. Figures were generated using XtalView (McRee, 1999), MOLSCRIPT (Kraulis, 1991) and Raster3d (Merritt & Bacon, 1997).

3. Results and Discussion

As of November 1, 2017, models for 215 GPCR crystal structures were available in the PDB. If two structures were of the same GPCR with similar unit cell dimensions and identical space group assignments, they were considered isomorphous. For each set of isomorphous structures, the one with the highest resolution was chosen as the exemplar for that crystal form. The assignment of isomorphous structures was not confirmed by comparison of diffraction patterns.

There are 121 unique crystal forms, some of which contain more than one molecule in the asymmetric unit, and this leads to 173 crystallographically unique GPCR molecules, i.e., GPCRs found in different packing environments. The number of close neighbours for each of those varies from 0 to

12 GPCR molecules. (For some of the structures where a GPCR is co-crystallized with other proteins, e.g., its G protein or a crystallization chaperone, there may be no or few GPCR-GPCR interactions.) A 400 $Å^2$ cutoff in buried solvent accessible surface areas (bSAS) per protein molecule limited the pairs of GPCRs for further consideration to 319 (out of 1033 possible) even though the cutoff is significantly smaller than the bSAS values for biologically significant oligomers (Janin, 1997).

The pairs of GPCRs were inspected visually and classified into four groups, parallel dimers, antiparallel dimers, crisscross dimers, and others (see Table 1). 71 pairs contained GPCRs oriented parallel to one another as you would expect for pairs that could possibly interact within a membrane. The exact orientation of these molecules with respect to a membrane is unknown, as is the membrane's location relative to the long axis of the molecules. The membrane is assumed to be roughly perpendicular to the axes of the transmembrane helices. In that case, the molecules in these "parallel" orientations would have their N- termini on one side of the membrane and their C-termini on the other.

137 of the interfaces involve pairs of receptors with the helices of one GPCR opposite in orientation relative to the other GPCR. Twenty interfaces contain molecules with their transmembrane domains roughly perpendicular to each other. Finally, there are 91 interfaces not involving contacts between the transmembrane domains. Many of the crystal structures are of GPCRs fused with other proteins to enhance their stability and/or crystallization properties. The interactions holding the crystals together in some cases are between the intra- and extra-cellular loops and the fusion domains. Some of these represent modes of interaction that might be found in native membranes, but they have been omitted from this study.

The 71 interfaces with GPCRs in parallel orientations will be called dimers for convenience, but it should be remembered that it is unknown if they form stable complexes in membrane environments. The molecules forming each dimer are listed in Tables 2 and 3 along with information allowing their

identification in the PDB. The first molecule listed for a dimer is considered the base or central molecule used for superpositions of the dimers.

The GPCRs in the parallel dimers are related by various rotations and translations. Seven pairs involve proteins related by translational symmetry, see Table 2. Two of these are only approximately translational symmetry with 2.2° rotations between the GPCRs. Also, four of these pairs are listed twice in Table 2 because both molecules forming the interface bury more than 400 $Å^2$ of bSAS. The interactions involved in these pairs are heterologous interactions, and when repeated, lead to infinite oligomers, not discrete dimers. However, these arrays might account for those observed for rhodopsin in native membranes (Liang *et al.*, 2003).

There are 18 parallel interfaces involving molecules related by approximate or exact three-, four-, and six-fold rotational axes perpendicular to the assumed membrane plane. There are three interfaces between molecules related by an approximate six-fold rotation axes, and one with exact six-fold symmetry. Four interfaces have approximate four-fold symmetry, and one has exact three-fold rotational symmetry. The exact rotation axes result in a cyclic hexamer or cyclic trimer, while the others do not form closed cyclic oligomers. These interactions are heterologous, so again the interfaces appear twice in Table 2.

The 42 remaining parallel interfaces contain GPCRs with transmembrane domains related by two-fold rotational symmetry axes perpendicular to the membrane plane. Crystallographic two-fold axes relate the GPCRs in 20 of these interfaces, and because the interfaces were generated for each of the crystallographically unique GPCRs, these interfaces appear only once in Table 3.

Twenty-two of the pairs involve non-crystallographic two-fold axes, and appear twice in the table. Strictly speaking, the interactions between the molecules in these dimers are heterologous. The two molecules in a dimer are not crystallographically identical, and the inter-protein interactions are not entirely symmetric. However, most of the angles of rotation relating the pairs of molecules are close to 180° (the largest deviation from 180° being 3.4°). Comparison of the bSAS for the molecules in these dimers show that for eight of the pairs, the difference in bSAS between the two interacting

molecules is less than 5% of the larger bSAS value. The molecules in these eight pairs appear to be nearly identical, so the one with the larger bSAS, has been used as the archetype for this dimer. For three of the interfaces (labelled 13, 21, and 27 in Table 3), larger differences in the bSAS for the molecules involved indicate that these interactions are more heterologous. To avoid over-counting of particular structures, only the GPCR with the larger bSAS will be considered further.

Figure 1 displays the result of superposing the 31 dimers listed in Table 3 that contain GPCRs related by two-fold rotation axes. The dimers were oriented by superposing the helices of each base molecule on the transmembrane helices of chain A of PDB entry 4X1H (Blankenship *et al.*, 2015) (opsin). A line connecting the centres of mass of the molecules in each pair was generated (see Figure 1A), and all 31 lines are shown in Figure 1B.

Dimers 1-13 (see listing in Table 3) form a cluster on the right of Figure 1B and contain receptors interacting mainly through helices TM1, TM2 and H8. Those on the left (14-31) are formed by interactions between helices TM3, TM4, TM5, and TM6. Table 4 lists the helices in the base molecules forming contacts in the dimer interfaces, and Table 5 lists the specific residues in the base molecules involved in each interface.

Identification of these general inter-helical interactions is not a new observation. Katritch, Cherezov and Stevens commented on several crystallographic dimers (Katritch *et al.*, 2013), and Baltoumas, Theodoropoulou and Hamodrakas included 16 crystallographic and computationally modelled dimers in their molecular dynamics study (Baltoumas *et al.*, 2016). The systematic search described here provides additional crystallographic examples of possible dimers. This larger set of examples shows the range of structures in the two clusters of dimers.

While the subunits in dimers 1-13 mainly interact via helices TM1, TM2 and H8, the relative orientation of the two-fold rotation axes relating the subunits in these dimers varies across the set. The subunits in dimers 1, 2, 3, 4, and 5 are arranged such that their two-fold axes are parallel to the long axes of the central receptor shown in Figure 1. Figure 2A is a view of dimer 4, looking

approximately down its two-fold rotation axis and is representative of this group of dimers. In this group, H8 from the left subunit is above that from the right subunit, see Figure 2B.

Dimers 6, 10, and 11 form another group with their two subunits twisted about the line between their centres when compared to the dimers in the first group (compare Figure 2C and 2a). As seen for dimer 6, the positions of H8 switch such that H8 from the left subunit is now below that from the right (Figure 2D). This structural difference positions the opposite side of the helix for subunit-subunit interactions compared to the dimers represented in Figure 2A.

A third set of dimers (7, 8, and 9) also contain subunits twisted about their line of centres relative to the first group (see Figure 2E), however, the sense of this twist is opposite to that of the second group. Associated with this different twist, H8 from the left subunit is again above that from the right (see Figure 2F). In dimers 12 and 13, there are no H8 helices, and this relaxes any restraint the helix places on subunit-subunit orientation. The connection between the orientation of the subunits and the position of H8 in the interface was made by Baltoumas, *et al*. (Baltoumas *et al.*, 2016), and the role of H8 in GPCR functioning has been noted (Sato *et al.*, 2016) with a focus on its interactions with other structural elements of its GPCR and on interactions between the GPCR and G proteins. It is also possible that amino acid sequence differences or physical conditions controlling helix folding of H8 might modulate signalling by affecting the role of H8 in the dimer interface.

On the other side of Figure 1B, the interfaces for dimers 14-31 are formed by inter-helical interactions involving TM3, TM4, TM5, and/or TM6 (see Figure 3 and Table 4). These structures cover a broad range of orientations, but they can also be grouped according to the locations of the two-fold rotation axes relating their subunits. The transmembrane helices in the subunits for these dimers are all roughly perpendicular to the membrane plane, but the rotation axes are found at different positions around the surface of the central molecule. This results in a systematic variation in the helices forming the dimer interactions (see Figure 3). Dimer 18 is representative of dimers 16-20 (see Figure 3A) where TM3, TM4 and TM5 are found at its interface. Dimer 24 is near the centre of dimers 21-27 (Figure 3B) where TM6 joins the set of interacting helices. Finally, for dimers 28 (Figure 3C), the

dimeric interface has moved along the surface to the point where neither TM4 nor TM6 makes contacts between the subunits. As is the case for dimers 1-13, considerable structural variation is found in interfaces for dimers 14-31, enough to provide several possible beginning points for homology modelling projects.

The residues in the transmembrane helices in the dimer interfaces are listed in Table 5. As expected for interactions between transmembrane helices, most of the residues involved are hydrophobic. At the ends of the helices, hydrophilic residues can form hydrogen bonds with other polar groups, and a few polar residues are also found in the central parts of the helices. Identification of residue positions that might be crucial for inter-subunit interactions is complicated by multiple occurrences of particular GPCRs in Table 5. For example, while residue position 1x40 (GPCRdb numbering (Isberg *et al.*, 2016)) is located in the interfaces of nine dimers, if β_1 adrenergic receptor and rhodopsin are counted only once, that number drops to five. Similarly, counting of the CXCR4 dimers only once significantly changes the number of times residues such as 3x51 or 5x38 are found at dimer interfaces.

While the orientation of the GPCRs in the interfaces reported here is consistent with them being in natural membranes, it is not clear that the observed inter-GPCR interactions are strong enough to be biologically relevant. Contributions of "core" residues in stabilizing inter-molecular contacts are major considerations in the eppic webserver (http://www.eppic-web.org/ewui/#) (Duarte *et al.*, 2012) designed to determine oligomeric states of membrane proteins. Most of the dimers listed in Table 3 have small bSAS, and there are few, if any, "core" residues in their interfaces. eppic suggests that the interfaces found in the 31 possible dimers are characteristic of crystal packing interfaces and not biologically relevant ones. Post-translational modifications and bound ligands further complicate this issue since they can stabilize the dimer interactions. Views of the interactions of these moieties with GPCRs are difficult to find since only a few of the low or moderate resolution crystal structure models include these group.

While none of the entries in Table 3 appear to involve extensive biologically relevant interfaces, it is noteworthy that CXCR4 appears in the table six times (dimers 21-24, 26, 27). As noted in the original

structure reports (Wu *et al.*, 2010, Qin *et al.*, 2015), a CXCR4 dimer is found in six different crystal packing arrangements, i.e., six different crystal forms. The six CXCR4 entries in Table 3 form a tight cluster in Figure 1B, and the structures are similar (see Figure 3B). These dimers make use of TM3, TM4, TM5, and TM6 in their inter-subunit interfaces.

Another receptor that appears several times in Table 3 is the β_1-adrenergic receptor (Huang *et al.*, 2013, Warne *et al.*, 2008, Moukhametzianov *et al.*, 2011, Miller-Gallacher *et al.*, 2014). In dimers 5, 6, and 11, TM1 and TM2 form the major interactions between the subunits. Dimers 6 and 11 are similar, but their subunits are oriented differently from those in dimer 5 (see Figure 2). β_1-adrenergic receptor dimers can also be formed by interactions using TM3, TM4 and TM5 (dimer 25). As opposed to the case of CXCR4 where the same interaction mode between GPCRs is seen in several crystal packing arrangements, fundamentally different dimers of β_1-adrenergic receptor need to be considered for studies of its oligomerization.

Rhodopsin/opsin dimers appear four times in Table 3 (numbers 1, 7, 8, and 9. Dimer 1 is formed by subunits that are nearly aligned. Dimers 7, 8, and 9 are similar in structure with subunits twisted relative to one another (Figure 2E). TM1 and TM2 form part of the subunit interfaces in all four dimers. Residues from TM6, TM7 and H8 are found at the interface in dimer 1, while dimer 8 also makes use of TM7 and H8 in its dimer interface. Low resolution electron microscopic, computational (PDB entry 1N3M), crosslinking, and mutagenesis studies (Liang *et al.*, 2003, Jastrzebska *et al.*, 2011, Jastrzebska *et al.*, 2016) resulted in the development and support of a rhodopsin dimer (PDB entry 1N3M) that utilizes TM4 and TM5 in the dimer interface. While this type of dimer is not consistent with the pairs seen in the rhodopsin/opsin crystal structures, it is like dimers 17-25.

4. Conclusions

Two major types of GPCR dimers deduced from their crystal structures have been identified by others (Katritch *et al.*, 2013, Baltoumas *et al.*, 2016). Previous studies have focused on particular receptors and their possible oligomers. What is unclear from the published records is whether all packing interactions in known GPCR crystal structures have been considered in

those studies. The larger number of experimentally determined GPCR crystal structures available now provides an opportunity to see how varied the members of those clusters are.

In the case of the dimers formed by interactions involving TM1 and TM2, twisting of the subunits around the line between their centres affects the overall relative orientations of the subunits. In addition, this has a major effect on H8 and how it interacts with other parts of its own GPCR and/or its dimeric mate. These structural differences might be associated with the effects of H8 on GPCR function.

Because of the recurring CXCR4 dimers and the rhodopsin modelling, the TM3-6 interface has been the focus of much attention. However, not all GPCR dimers based on this interface make use of it in the same way. There is a continuum of structures using portions of this interface because it covers such a large part of the protein's transmembrane surface. The variation can be seen in Table 4 where dimers 14-18 mainly have TM3-5 between the subunits, dimers 19-29 use TM3-6, and finally dimers 30-31 are stabilized by interactions of TM5 and TM6. The different pieces of this surface used in forming dimers is a complication of some importance because it expands the number of possible beginning models for computational studies of GPCR dimerization.

Examination of all the dimeric crystal packing interactions also shows that only certain parts of the transmembrane surfaces of GPCRs are involved in forming parallel dimers. This appears as the systematic split in the dimers in Figure 1B. It is apparent from comparing interfaces from the crystal structures that not all combinations of transmembrane helices can lead to stable dimers. This restriction on which helices form dimeric interfaces is a powerful restraint to be considered in modelling GPCR dimers.

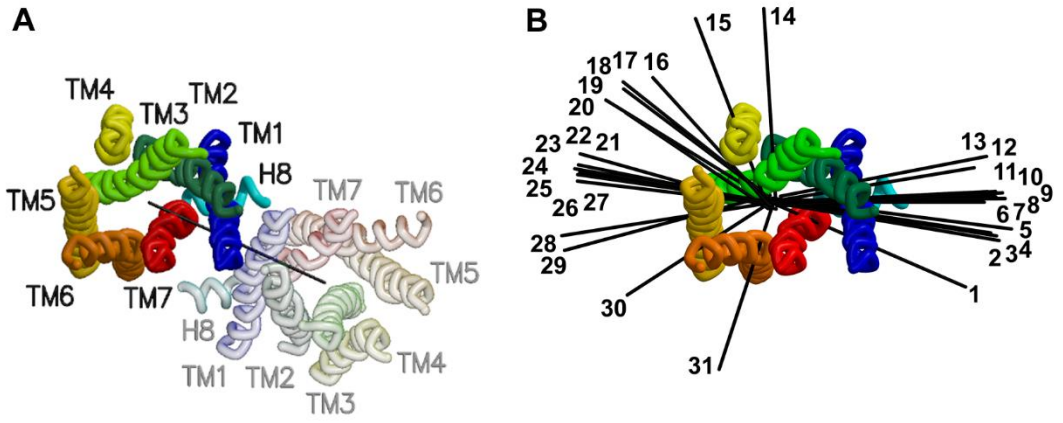

Figure 1 Schematic showing locations of lines-of-center of dimer subunits. (A) Two GPCRs in a dimer with a line joining their centers viewed perpendicular to the plane of the membrane. TM1 shown in blue, TM2 in dark green, TM3 in chartreuse, TM4 in yellow, TM5 in gold, TM6 in orange, TM7 in red, and H8 in cyan. The colors for the second subunit are the same, but in transparent mode. (B) Similar plot, but showing the lines connecting the centers of each of the 31 parallel dimers showing two-fold rotational symmetry (see Table 3).

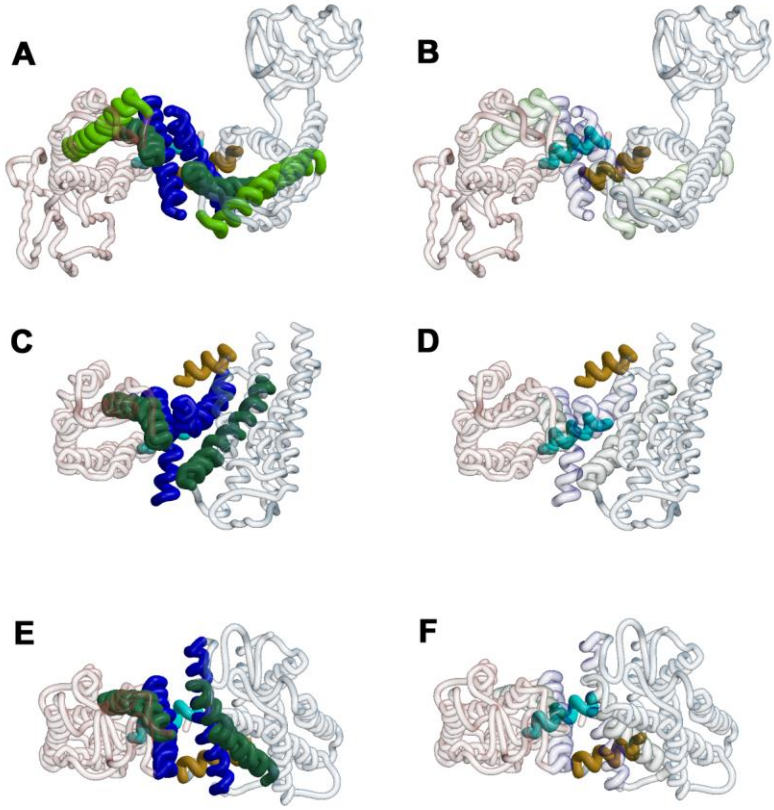

Figure 2 Selected dimers formed using TM1-3 at their interfaces. The central and second molecules are shown as transparent red or blue alpha carbon tracings. Transmembrane helices at the interface are shown in bold colors. TM1 shown in blue, TM2 in dark green, TM3 in chartreuse. H8 from the central and second molecules shown in cyan and brown. (A) Dimer 4 looking down on the extracellular side of the GPCRs. (B) Same view of dimer 4, but clipped to show H8. (C) Dimer 6. (D) Same view, as in (B). (E) Dimer 7. (F) Same view, as in (B).

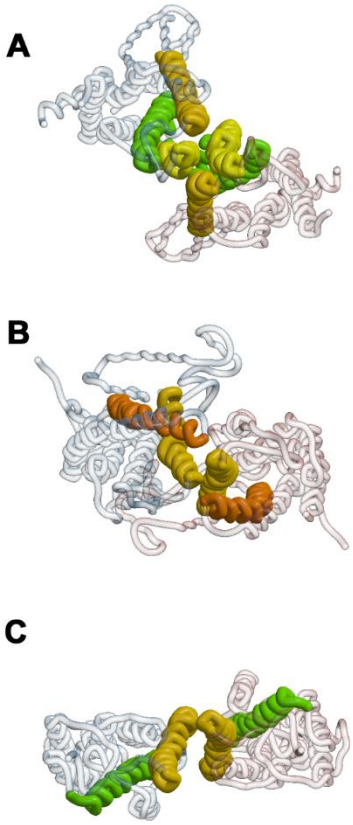

Figure 3 Selected dimers formed using TM3-6 at their interfaces. The central molecule is shown as a transparent red alpha carbon tracing. The second molecule is shown in transparent blue. Transmembrane helices at the interface are shown in bold colors. TM3 in chartreuse, TM4 in yellow, TM5 in gold, TM6 in orange. (A) Dimer 18 looking down on the extracellular side of the GPCRs. (B) Dimer 24. (C) Dimer 28.

Table 1 Crystal forms and GPCR-GPCR interactions. The PDB identification code for the exemplar structure is given for each crystal form. The number of packing interfaces is provided for each crystallographically unique GPCR chain in that structure. The numbers of parallel, antiparallel, crisscross and other interfaces as well as the interfaces with bSAS values less than 400 Å^2 are also listed. The last column contains PDB identification codes for isomorphous structures.

Crystal form	Molecule	PDB code	Unit cell (a, b, c, α, β, γ) (Å, °) and space group	Resolution, (Å)	Reference	GPCR chain	# interfaces	# parallel	# antiparallel	#crisscross	# other	# too small	Isomorphous PDB entries
tc-01	β_1 adrenergic receptor	2VT4	55.500 86.800 95.500 67.60 73.30 85.80 P1	2.7	(Warne *et al.*, 2008)	A	7	1	0	1	1	4	
						B	7	0	0	1	1	5	
						C	7	0	0	1	1	5	
						D	7	1	0	1	1	4	
tc-02	CXCR4 chemokine receptor	3OE8	69.369 76.602 91.719 96.00 97.78 97.38 P1	3.1	(Wu *et al.*, 2010)	A	9	3	0	0	0	6	
						B	9	3	0	0	0	6	
						C	8	2	0	0	0	6	
tc-03	CXCR4 chemokine receptor	3OE9	72.497 72.739 84.273 64.66 73.93 61.31 P1	3.1	(Wu *et al.*, 2010)	A	6	1	0	0	1	4	
						B	6	1	0	0	0	5	
tc-04	M_3 muscarinic acetylcholine receptor	4DAJ	54.770 61.310 176.910 85.87 89.90 84.90 P1	3.4	(Kruse *et al.*, 2012)	A	4	0	1	0	1	2	
						B	4	0	1	0	0	3	
						C	4	0	1	0	0	3	
						D	4	0	1	0	1	2	
tc-05	P2Y1 receptor	4XNW	40.670 64.970 77.570 101.82 95.70 100.85 P1	2.7	(Zhang, Gao, *et al.*, 2015)	A	7	0	2	0	1	4	
						C	7	0	2	0	1	4	
tc-06	smoothened receptor	5L7I	52.820 71.290 107.020 91.53 98.20 105.92 P1	3.3	(Byrne *et al.*, 2016)	A	12	0	1	0	1	10	
						B	10	0	1	0	0	9	
tc-07	CCR9 chemokine receptor	5LWE	62.571 66.197 68.424 74.02 64.72 62.29 P1	2.8	(Oswald *et al.*, 2016)	A	5	2	0	0	1	2	
						B	7	2	0	0	1	4	
tc-08	GLP-1 receptor	5VEW	64.770 66.430 83.440 90.54 90.18 107.73 P1	2.7	(Song *et al.*, 2017)	A	5	0	2	0	0	3	5VEX
						B	5	0	2	0	0	3	
tc-09	protease-activated receptor 2	5NDD	37.109 62.264 87.341 104.88 90.88 96.89 P1	2.8	(Cheng, Fiez-Vandal, *et al.*, 2017)	A	8	1	0	0	0	7	5NDZ
mo-01	β_1 adrenoceptor	4AMJ	90.056 62.196 100.926 90.00 109.17 90.00 $P2_1$	2.3	(Warne *et al.*, 2012)	A	4	0	0	1	3	0	2Y00 2Y01 2Y02 2Y03 2Y04 3ZPQ 3ZPR
						B	4	0	0	1	2	1	

mo-02	β_1 adrenergic receptor	2YCW	89.398 57.056 109.542 90.00 113.52 90.00 $P2_1$	3.0	(Moukhametzianov *et al.*, 2011)	A	4	0	0	1	2	1	4AMI
						B	4	0	1	0	2	1	
mo-03	M_2 muscarinic acetylcholine receptor	3UON	78.170 47.260 88.120 90.00 109.70 90.00 $P2_1$	3.0	(Haga *et al.*, 2012)	A	6	0	2	0	0	4	
mo-04	A_{2A} adenosine receptor	3EML	47.736 76.932 86.553 90.00 101.32 90.00 $P2_1$	2.6	(Jaakola *et al.*, 2008)	A	10	0	2	0	0	8	3QAK
mo-05	CXCR4 chemokine receptor	3ODU	64.540 83.692 119.995 90.00 102.17 90.00 :%s/ $P2_1$	2.5	(Wu *et al.*, 2010)	A	9	1	4	0	0	4	
						B	7	1	4	0	0	2	
mo-06	β_2 adrenergic receptor – Gs complex	3SN6	119.339 64.555 131.240 90.00 91.67 90.00 $P2_1$	3.2	(Rasmussen, DeVree, *et al.*, 2011)	R	0	0	0	0	0	0	
mo-07	nociceptin/ orphanin FQ peptide receptor	5DHG	42.079 171.696 66.491 90.00 103.25 90.00 $P2_1$	3.0	(Miller *et al.*, 2015)	A	4	0	3	0	0	1	4EA3 5DHH
						B	6	0	3	0	1	2	
mo-08	smoothened receptor	4O9R	40.500 157.300 52.400 90.00 97.00 90.00 $P2_1$	3.2	(Weierstall *et al.*, 2014)	A	6	0	0	0	1	5	
mo-09	neurotensin receptor	4GRV	49.960 69.619 97.550 90.00 101.75 90.00 $P2_1$	2.8	(White *et al.*, 2012)	A	10	0	2	0	0	8	
mo-10	A_{2A} adenosine receptor	4UHR	60.407 59.187 65.058 90.00 92.83 90.00 $P2_1$	2.6	(Lebon *et al.*, 2015)	A	10	0	2	0	0	8	
mo-11	smoothened receptor	4JKV	60.407 59.187 65.058 90.00 92.83 90.00 $P2_1$	2.45	(Wang, Wu, *et al.*, 2013)	A	6	1	0	0	1	4	
						B	8	1	0	0	1	6	
mo-12	M_4 muscarinic acetylcholine receptor	5DSG	48.490 172.040 60.660 90.00 94.37 90.00 $P2_1$	2.6	(Thal *et al.*, 2016)	A	12	0	2	0	1	9	
						B	12	0	2	0	0	10	
mo-13	CB_1 cannabinoid receptor	5U09	50.652 80.381 81.178 90.00 91.72 90.00 $P2_1$	2.6	(Shao *et al.*, 2016)	A	10	0	0	0	0	10	
mo-14	angiotensin II type 2 receptor	5UNF	77.390 69.110 90.070 90.00 104.33 90.00 $P2_1$	2.8	(Zhang, Han, *et al.*, 2017)	A	9	0	1	0	0	8	5UNH
						B	9	0	3	0	0	6	
mo-15	smoothened receptor	5V56	40.590 349.540 61.760 90.00 101.10 90.00 $P2_1$	2.9	(Zhang, Zhao, *et al.*, 2017)	A	8	1	0	0	1	6	5V57
						B	10	0	0	0	2	8	
mo-16	glucagon receptor	5XEZ	72.610 245.330 96.150 90.00 90.01 90.00 $P2_1$	3.0	(Zhang, Qiao, *et al.*, 2017)	A	1	0	0	0	0	1	5XF1
						B	3	0	0	0	0	3	
mo-17	serotonin 2B receptor	5TUD	71.290 118.860 145.380 90.00 90.37 90.00 $P2_1$	3.0	(Ishchenko *et al.*, 2017)	A	3	0	2	0	0	1	
						D	3	0	2	0	0	1	
mo-18	free fatty acid receptor 1	5TZY	53.880 63.950 90.960 90.00 90.52 90.00 $P2_1$	3.22	(Lu *et al.*, 2017)	A	6	0	2	0	0	4	
mo-19	β_1 adrenergic receptor	2YCX	150.029 56.434 111.410 90.00 118.33 90.00 C2	3.25	(Moukhametzianov *et al.*, 2011)	A	6	0	0	1	1	4	
						B	6	0	0	1	1	4	

mo-20	β_1 adrenergic receptor	2YCY	184.760 56.161 89.778 90.00 111.27 90.00 C2	3.15	(Moukhametzianov *et al.*, 2011)	A	8	1	0	1	1	5	
						B	6	0	0	1	1	4	
mo-21	β_1 adrenergic receptor;	2YCZ	177.855 56.298 110.939 90.00 116.39 90.00 C2	3.65	(Moukhametzianov *et al.*, 2011)	A	7	0	0	1	0	6	
						B	6	0	0	1	0	5	
mo-22	A_{2A} adenosine receptor	2YDV	76.936 99.551 79.655 90.00 93.31 90.00 C2	2.6	(Lebon *et al.*, 2011)	A	8	0	0	0	3	5	2YDO
mo-23	CXCR4 chemokine receptor	3OE0	82.080 144.860 73.990 90.00 104.54 90.00 C2	2.9	(Wu *et al.*, 2010)	A	4	1	0	0	1	2	
mo-24	β_2 adrenoceptor	3P0G	236.686 45.660 71.375 90.00 102.34 90.00 C2	3.5	(Rasmussen, Choi, *et al.*, 2011)	A	4	0	2	0	0	2	
mo-25	A_{2A} adenosine receptor	3VG9	121.180 90.150 113.550 90.00 98.10 90.00 C2	2.7	(Hino *et al.*, 2012)	A	1	0	0	0	0	1	3VGA
mo-26	β_2 adrenergic receptor	2R4R	338.380 48.480 89.350 90.00 104.60 90.00 C2	3.4	(Rasmussen *et al.*, 2007)	A	2	0	0	0	0	2	2R4S 3KJ6
mo-27	β_2 adrenergic receptor	2RH1	106.318 169.240 40.154 90.00 105.62 90.00 C2	2.4	(Cherezov *et al.*, 2007)	A	9	0	0	0	0	9	5D5A 5D5B 5D6L
mo-28	μ-opioid receptor	4DKL	70.882 174.730 68.353 90.00 107.84 90.00 C2	2.8	(Manglik *et al.*, 2012)	A	5	2	0	0	1	2	
mo-29	smoothened receptor	4QIN	72.220 158.930 60.020 90.00 90.26 90.00 C2	2.6	(Wang *et al.*, 2014)	A	8	1	0	0	1	6	
mo-30	angiotensin receptor	4YAY	72.800 41.000 167.700 90.00 99.40 90.00 C2	2.9	(Zhang, Unal, Gati, *et al.*, 2015)	A	8	0	0	0	0	8	
mo-31	$P2Y_{12}$ receptor	4PY0	75.650 65.110 100.740 90.00 95.50 90.00 C2	3.1	(Zhang, Zhang, Gao, Paoletta, *et al.*, 2014)	A	6	0	3	0	0	3	
mo-32	δ-opioid receptor	4N6H	86.230 72.851 84.408 90.00 107.48 90.00 C2	1.8	(Fenalti *et al.*, 2014)	A	9	0	2	0	1	6	
mo-33	orexin receptor	4S0V	94.358 75.819 96.335 90.00 111.71 90.00 C2	2.5	(Yin *et al.*, 2015)	A	7	0	2	0	1	4	
mo-34	$P2Y_{12}$ receptor	4NTJ	98.650 156.430 47.770 90.00 111.08 90.00 C2	2.62	(Zhang, Zhang, Gao, Zhang, *et al.*, 2014)	A	8	0	0	0	0	8	
mo-35	free fatty acid receptor 1	5TZR	100.620 62.600 106.150 90.00 108.93 90.00 C2	2.2	(Lu *et al.*, 2017)	A	6	0	3	0	0	3	4PHU
mo-36	metabotropic glutamate receptor 5	4OO9	143.242 43.555 82.049 90.00 99.37 90.00 C2	2.6	(Dore *et al.*, 2014)	A	10	0	1	0	0	9	5CGC 5CGD
mo-37	M_3 muscarinic acetylcholine receptor	4U15	152.311 184.563 52.613 90.00 98.54 90.00 C2	2.8	(Thorsen *et al.*, 2014)	A	4	0	1	0	0	3	4U16
						B	4	0	1	0	0	3	
mo-38	δ-opioid receptor	4RWD	156.230 89.290 96.420 90.00 92.30 90.00 C2	2.7	(Fenalti *et al.*, 2015)	A	6	0	0	0	1	5	
						B	6	0	0	0	1	5	
mo-39	δ-opioid receptor	4RWA	160.549 86.121 94.684 90.00 92.21 90.00 C2	3.28	(Fenalti *et al.*, 2015)	A	6	0	0	0	1	5	

						B	6	0	0	0	1	5	
mo-40	5-hydroxy-tryptamine $_{1B}$ receptor	4IAR	195.290 45.500 74.280 90.00 95.45 90.00 C2	2.7	(Wang, Jiang, *et al.*, 2013)	A	4	0	2	0	0	2	
mo-41	β_1 adrenergic receptor	5F8U	229.660 79.590 69.040 90.00 101.83 90.00 C2	3.35	(Leslie *et al.*, 2015)	A	5	1	0	0	0	4	4GPO
						B	5	1	0	0	0	4	
mo-42	CB_1 cannabinoid receptor	5TGZ	116.560 52.630 143.630 90.00 111.14 90.00 C2	2.8	(Hua *et al.*, 2016)	A	6	0	0	0	1	5	
mo-43	smoothened receptor	5L7D	122.900 63.020 208.590 90.00 96.64 90.00 C2	3.2	(Byrne *et al.*, 2016)	A	9	0	2	0	1	6	
						B	8	0	0	0	1	7	
mo-44	apelin receptor	5VBL	150.580 44.300 79.450 90.00 114.87 90.00 C2	2.6	(Ma *et al.*, 2017)	B	4	0	1	0	1	2	
or-01	sphingosine 1-phosphate $_1$ receptor	3V2Y	107.940 69.700 81.930 90.00 90.00 90.00 $P2_12_12$	2.8	(Hanson *et al.*, 2012)	A	9	1	0	0	0	8	3V2W
or-02	β_2 adrenergic receptor	3PDS	282.440 40.040 65.210 90.00 90.00 90.00 $P2_12_12$	3.5	(Rosenbaum *et al.*, 2011)	A	7	0	0	0	1	6	
or-03	neurotensin receptor	5T04	104.190 75.710 83.200 90.00 90.00 90.00 $P2_12_12$	3.3	(Krumm *et al.*, 2016)	A	11	0	1	0	1	9	
or-04	protease-activated receptor 2	5NJ6	164.144 38.520 159.660 90.00 90.00 90.00 $P2_12_12$	4.0	(Cheng, Fiez-Vandal, *et al.*, 2017)	A	5	0	0	0	0	5	
or-05	β_1 adrenoceptor	4BVN	53.093 62.127 95.776 90.00 90.00 90.00 $P2_122_1$	2.1	(Miller-Gallacher *et al.*, 2014)	A	8	1	2	0	2	3	5A8E
or-06	neurotensin receptor	4XES	49.840 88.440 161.330 90.00 90.00 90.00 $P2_122_1$	2.6	(Krumm *et al.*, 2015)	A	5	0	0	0	0	5	4XEE
or-07	angiotensin II type 2 receptor	5UNG	70.260 78.790 93.410 90.00 90.00 90.00 $P\ 2_122_1$	2.8	(Zhang, Han, *et al.*, 2017)	B	10	0	2	0	1	7	
or-08	CB_1 cannabinoid receptor	5XRA	66.050 75.870 138.900 90.00 90.00 90.00 $P2_122_1$	2.8	(Hua *et al.*)	A	9	0	2	0	1	6	5XR8
or-09	corticotropin-releasing factor receptor 1	4K5Y	86.559 123.968 166.834 90.00 90.00 90.00 $P22_12_1$	2.98	(Hollenstein *et al.*, 2013)	A	5	0	1	0	0	4	
						B	6	1	1	0	0	4	
						C	3	2	0	0	0	1	
or-10	A_1 adenosine receptor	5UEN	96.492 112.960 124.171 90.00 90.00 90.00 $P22_12_1$	3.2	(Glukhova *et al.*, 2017)	A	5	1	0	0	0	4	
						B	4	0	0	0	0	4	
or-11	CCR5 chemokine receptor	5UIW	38.010 52.640 302.670 90.00 90.00 90.00 $P22_12_1$	2.2	(Zheng *et al.*, 2017)	A	6	2	0	0	0	4	
or-12	β_2 adrenergic receptor	5X7D	40.460 75.710 173.410 90.00 90.00 90.00 $P2_12_12_1$	2.7	(Liu *et al.*, 2017)	A	10	0	0	0	0	10	3D4S 3NY8 3NY9 3NYA
or-13	dopamine D3 receptor	3PBL	88.828 92.492 176.116 90.00 90.00 90.00 $P2_12_12_1$	2.89	(Chien *et al.*, 2010)	A	8	0	1	0	0	7	
						B	4	0	1	0	0	3	
or-14	κ-opioid receptor	4DJH	54.896 147.297 205.288 90.00 90.00 90.00 $P2_12_12_1$	2.9	(Wu *et al.*, 2012)	A	7	1	1	0	0	5	
						B	7	1	1	0	0	5	
or-15	smoothened receptor	4QIM	42.830 79.840 170.070 90.00 90.00 90.00 $P2_12_12_1$	2.61	(Wang *et al.*, 2014)	A	10	0	0	0	2	8	

or-16	protease-activated receptor 1	3VW7	44.044 71.460 172.187 90.00 90.00 90.00 $P2_12_12_1$	2.2	(Zhang *et al.*, 2012)	A	8	0	2	0	1	5	
or-17	β_2 adrenoceptor	4LDE	49.670 66.480 303.100 90.00 90.00 90.00 $P2_12_12_1$	2.79	(Ring *et al.*, 2013)	A	4	0	0	0	0	4	4QKX 4LDL 4LDO
or-18	β_2 adrenergic receptor	4GBR	51.382 71.376 161.370 90.00 90.00 90.00 $P2_12_12_1$	3.99	(Zou *et al.*, 2012)	A	4	0	1	0	1	2	note 1
or-19	glucagon receptor	4L6R	56.615 66.651 163.331 90.00 90.00 90.00 $P2_12_12_1$	3.3	(Siu *et al.*, 2013)	A	6	0	0	0	2	4	
or-20	A_{2A} adenosine receptor	4UG2	57.253 105.944 125.861 90.00 90.00 90.00 $P2_12_12_1$	2.6	(Lebon *et al.*, 2015)	A	5	1	1	0	0	3	
						B	3	1	1	0	0	1	
or-21	neurotensin receptor 1	3ZEV	58.550 90.180 209.360 90.00 90.00 90.00 $P2_12_12_1$	1.99	(Egloff *et al.*, 2014)	A	5	0	0	1	0	4	4BV0 4BWB
						B	3	0	0	1	0	2	
or-22	M_2 muscarinic acetylcholine receptor	4MQT	59.032 77.399 163.822 90.00 90.00 90.00 $P2_12_12_1$	3.7	(Kruse *et al.*, 2012)	A	2	0	0	0	0	2	
or-23	M_2 muscarinic acetylcholine receptor	4MQS	62.896 78.130 163.482 90.00 90.00 90.00 $P2_12_12_1$	3.5	(Kruse *et al.*, 2012)	A	2	0	0	0	0	2	
or-24	neurotensin receptor 1	4BUO	63.310 89.400 212.130 90.00 90.00 90.00 $P2_12_12_1$	2.75	(Egloff *et al.*, 2014)	A	6	0	0	1	1	4	
						B	4	0	0	1	1	2	
or-25	metabotropic glutamate receptor 1	4OR2	67.361 86.552 168.277 90.00 90.00 90.00 $P2_12_12_1$	2.8	(Wu *et al.*, 2014)	A	7	1	1	0	0	5	
						B	7	1	1	0	0	5	
or-26	CCR5 chemokine receptor	4MBS	67.361 86.552 168.277 90.00 90.00 90.00 $P2_12_12_1$	2.71	(Tan *et al.*, 2013)	A	6	2	0	0	1	3	
						B	6	2	0	0	1	3	
or-27	lysophosphatidic acid receptor 1	4Z35	34.610 112.400 155.670 90.00 90.00 90.00 P 21 21 21	2.9	(Chrencik *et al.*, 2015)	A	8	2	0	0	0	6	4Z34 4Z36
or-28	M_1 muscarinic acetylcholine receptor	5CXV	58.053 72.186 175.688 90.00 90.00 90.00 $P2_12_12_1$	2.7	(Thal *et al.*, 2016)	A	4	0	2	0	0	2	
or-29	human rhodopsin	5W0P	109.240 109.240 452.640 90.00 90.00 90.00 $P2_12_12_1$	3.0	(Zhou *et al.*, 2017)	A	8	1	0	0	1	6	4ZWJ 5DGY
						B	6	0	1	0	1	4	
						C	6	0	1	0	0	5	
						D	8	0	1	0	1	6	
or-30	OX1 orexin receptor	4ZJ8	63.242 64.992 181.478 90.00 90.00 90.00 $P2_12_12_1$	2.75	(Yin *et al.*, 2016)	A	4	0	1	0	0	3	4ZJC
or-31	A_{2A} adenosine receptor – mini Gs complex	5G53	90.632 111.814 161.304 90.00 90.00 90.00 $P2_12_12_1$	3.4	(Carpenter *et al.*, 2016)	A	1	0	0	0	1	0	
						B	1	0	0	0	1	0	
or-32	CCR2 chemokine receptor	5T1A	59.230 64.690 169.980 90.00 90.00 90.00 $P2_12_12_1$	2.81	(Zheng *et al.*, 2016)	A	6	0	2	0	0	4	
or-33	lysophosphatidic acid	5XSZ	55.880 65.020 160.650 90.00 90.00 90.00 $P2_12_12_1$	3.2	(Taniguchi *et al.*, 2017)	A	4	0	2	0	0	2	

	receptor 6A												
or-34	glucagon receptor	5EE7	37.583 71.476 183.108 90.00 90.00 90.00 $P2_12_12_1$	2.5	(Jazayeri *et al.*, 2016)	A	10	1	2	0	0	7	
or-35	β_2 adrenergic receptor	5JQH	43.924 164.486 218.749 90.00 90.00 90.00 $P2_12_12_1$	3.2	(Staus *et al.*, 2016)	A	2	0	1	0	0	1	
						B	2	0	1	0	0	1	
or-36	5-hydroxy-tryptamine $_{1B}$ receptor	4IAQ	84.740 192.579 74.341 90.00 90.00 90.00 C222	2.8	(Wang, Jiang, *et al.*, 2013)	A	4	0	2	0	0	2	
or-37	A_1 adenosine receptor	5N2S	70.273 111.658 160.543 90.00 90.00 90.00 C222	3.3	(Cheng, Segala, *et al.*, 2017)	A	6	2	0	0	0	4	
or-38	squid rhodopsin	2ZIY	84.319 108.746 142.165 90.00 90.00 90.00 $C222_1$	3.7	(Shimamura *et al.*, 2008)	A	2	1	1	0	0	0	
or-39	smoothened receptor	4N4W	84.640 110.880 145.210 90.00 90.00 90.00 $C222_1$	2.8	(Wang *et al.*, 2014)	A	8	0	0	0	1	7	
or-40	A_{2A} adenosine receptor	5NM4	39.890 179.150 141.200 90.00 90.00 90.00 $C222_1$	1.7	(Weinert *et al.*, 2017)	A	6	0	1	0	0	5	4EIY 5JTB 5MZJ 5MZP 5N2R 5NLX 5NM2 5UVI 5IU4 5IU7 5IU8 5IUA 5IUB 5K2A 5K2B 5K2C 5K2D
or-41	human cyto-megalovirus GPCR US28	4XT3	59.900 192.700 94.400 90.00 90.00 90.00 $C222_1$	3.8	(Burg *et al.*, 2015)	A	3	0	2	0	0	1	
or-42	5-hydroxy-tryptamine $_{2B}$ receptor	4IB4	60.571 119.750 170.607 90.00 90.00 90.00 $C222_1$	2.7	(Wacker *et al.*, 2013)	A	7	0	3	0	0	4	4NC3 5TVN
or-43	$P2Y_{12}$ receptor	4PXZ	65.110 104.170 169.430 90.00 90.00 90.00 $C222_1$	2.5	(Zhang, Zhang, Gao, Paoletta, *et al.*, 2014)	A	6	0	2	0	0	4	
or-44	endothelin ET_B receptor	5GLH	72.970 172.970 109.350 90.00 90.00 90.00 $C222_1$	2.8	(Shihoya *et al.*, 2016)	A	7	0	0	0	0	7	
or-45	endothelin ET_B receptor	5X93	74.130 147.480 108.380 90.00 90.00 90.00 $C222_1$	2.2	(Shihoya *et al.*, 2017)	A	9	0	2	0	1	6	5GLI
or-46	D_4 dopamine receptor	5WIU	67.688 164.047 84.129 90.00 90.00 90.00 $C222_1$	1.96	(Wang *et al.*, 2017)	A	9	0	1	0	1	7	5WIV
or-47	CXCR4 chemokine receptor	3OE6	71.121 78.711 240.592 90.00 90.00 90.00 I222	3.2	(Wu *et al.*, 2010)	A	7	1	3	0	0	3	
or-48	A_{2A} adenosine receptor	3UZA	111.814 111.896 125.841 90.00 90.00 90.00 I222	3.27	(Congreve *et al.*, 2012)	A	3	0	0	0	2	1	3PWH 3REY 3RFM 3UZC
or-49	CXCR4 chemokine receptor	4RWS	82.320 121.827 189.766 90.00 90.00 90.00 I222	3.1	(Qin *et al.*, 2015)	A	4	1	0	0	0	3	
or-50	μ-opioid receptor	5C1M	44.430 144.000 209.900 90.00 90.00 90.00 $I2_12_12_1$	2.1	(Huang *et al.*, 2015)	A	4	1	1	0	0	2	
te-01	bovine rhodopsin	1U19	96.680 96.680 150.200 90.00 90.00 90.00	2.2	(Okada *et al.*, 2004)	A	6	0	1	0	2	3	1F88 1HZX

			$P4_1$										1L9H 2G87 2HPY 2PED 3OAX
						B	6	0	1	0	3	2	
te-02	M_3 muscarinic acetylcholine receptor	4U14	54.952 54.952 348.030 90.00 90.00 90.00 $P4_12_12$	3.57	(Thorsen *et al.*, 2014)	A	4	0	1	0	1	2	
te-03	A_{2A} adenosine receptor	5UIG	131.222 131.222 89.714 90.00 90.00 90.00 $P4_12_12$	3.5	(Sun *et al.*, 2017)	A	7	0	1	0	0	6	
te-04	human cyto-megalovirus GPCR US28	4XT1	81.024 81.024 231.303 90.00 90.00 90.00 I4	2.89	(Burg *et al.*, 2015)	A	4	0	0	0	0	4	
te-05	histamine H_1 receptor	3RZE	88.144 88.144 331.654 90.00 90.00 90.00 I422	3.1	(Shimamura *et al.*, 2011)	A	8	0	0	0	0	8	
tg-01	angiotensin II type-1 receptor	4ZUD	41.200 41.200 251,160 90.00 90.00 120.00 $P3_2$	2.8	(Zhang, Unal, Desnoyer, *et al.*, 2015)	A	8	0	0	0	0	8	
tg-02	bovine rhodopsin	2I36	159.866 159.866 142.150 90.00 90.00 120.00 $P3_112$	4.1	(Salom *et al.*, 2006)	A	2	1	0	0	1	0	2I37
						B	2	1	0	0	1	0	
						C	3	1	0	0	1	1	
tg-03	δ-opioid receptor	4EJ4	73.278 73.278 266.653 90.00 90.00 120.00 $P3_121$	3.4	(Granier *et al.*, 2012)	A	3	0	2	0	0	1	
tg-04	GLP-1 receptor	5NX2	94.435 94.435 163.905 90.00 90.00 120.00 $P3_121$	3.7	(Jazayeri *et al.*, 2017)	A	5	0	1	0	2	2	
tg-05	bovine opsin	5TE5	81.725 81.725 200.012 90.00 90.00 120.00 $P3_121$	4.0	(Gulati *et al.*, 2017)	A	5	0	0	0	0	5	
tg-06	endothelin ET_B receptor	5XPR	74.720 74.720 218.870 90.00 90.00 120.00 $P3_221$	3.6	(Shihoya *et al.*, 2017)	A	5	0	2	0	1	2	
rh-01	$P2Y_1$ receptor	4XNV	66.270 66.270 239.070 90.00 90.00 120.00 R3	2.2	(Zhang, Gao, *et al.*, 2015)	A	8	2	0	0	0	6	
rh-02	bovine opsin	4X1H	242.136 242.136 109.721 90.0 90.00 120.00 R32	2.29	(Blankenship *et al.*, 2015)	A	4	1	0	0	1	2	2X72 3CAP 3DQB 3PQR 3PXO 4A4M 4BEY 4BEZ 4J4Q 4PXF 5DYS note 2
rh-03	bovine rhodopsin	2I35	277.534 277.534 66.321 90.00 90.00 120.00 R32	3.8	(Salom *et al.*, 2006)	A	3	1	0	0	1	1	
he-01	corticotropin-releasing factor receptor 1	4Z9G	189.359 189.359 88.575 90.00 90.00 120.00 P6	3.18	(Dore *et al.*, 2017)	A	7	2	0	0	0	5	
						B	7	2	0	0	0	5	
						C	2	2	0	0	0	5	
he-02	squid rhodopsin	2Z73	122.550 122.550 158.740 90.00 90.00 120.00 $P6_2$	2.5	(Murakami & Kouyama, 2008)	A	4	1	1	0	1	1	3AYM 3AYN 4WW3
						B	4	1	1	0	1	1	

he-03	bovine rhodopsin	3C9L	103.820 103.820 76.590 90.00 90.00 120.00 $P6_4$	2.65	(Stenkamp, 2008)	A	5	0	1	2	0	2	note 3
he-04	bovine rhodopsin	3C9M	109.300 109.300 77.700 90.00 90.00 120.00 $P6_4$	3.4	(Stenkamp, 2008)	A	5	0	1	1	0	3	note 4

Note 1. The fusion domain for PDB entry 4GBR is listed as chain B. Chain B was combined with chain A for this study.

Note 2. PDB entry 3CAP is included in crystal form rh-02. An alternative interpretation of that structure involves converting non-crystallographic symmetry to crystallographic symmetry operations.

Note 3. PDB entry 3C9L is an alternative model for PDB entry 1GZM.

Note 4. PDB entry 3C9M is an alternative model for PDB entry 2J4Y.

Table 2 Interfaces between parallel GPCRs not related by two-fold rotational symmetry. The central subunit is positioned as in the deposited PDB file. The symmetry operation is applied to the other chain's fractional coordinates. The rotation column is derived from the transformation relating the subunits' transmembrane helices. The buried solvent accessible surface (bSAS) values are for the central molecule and its transmembrane helices. Non-crystallographic (ncs) and crystallographic symmetry (cryst) are noted. Entries with no molecule name listed are the opposing faces for the interfaces listed immediately before them.

Molecule	PDB code	Reference	Central subunit	Second subunit	Symmetry operation	Rotation (°)	bSAS total	bSAS transmembrane helices		Symmetry
CXCR4 chemokine receptor	3OE8	(Wu *et al.*, 2010)	C	A	x,y+1,z	91.9	852.2	684.1		ncs
			A	C	x,y-1,z	91.9	761.1	507.0		ncs
corticotropin-releasing factor receptor 1	4K5Y	(Hollenstein *et al.*, 2013)	B	C	-x-1, y+1/2, 1/2-z	64.8	811.9	811.9		ncs
			C	B	-x-1,y-1/2,1/2-z	64.8	798.7	762.0		ncs
CXCR4 chemokine receptor	3OE8	(Wu *et al.*, 2010)	A	B	x,y,z	85.3	746.9	579.0		ncs
			B	A	x,y,z	85.3	657.6	596.7		ncs
CCR5 chemokine receptor	4MBS	(Tan *et al.*, 2013)	B	A	x+1,y,z	2.2	724.4	499.2		ncs
			A	B	x-1,y,z	2.2	656.3	574.1		ncs
CCR5 chemokine receptor	4MBS	(Tan *et al.*, 2013)	A	B	x,y,z	2.2	672.3	560.3		ncs
			B	A	x,y,z	2.2	660.0	625.3		ncs
lysophosphatidic acid receptor 1	4Z35	(Chrencik *et al.*, 2015)	A	A	x-1,y,z	0.0	668.8	591.3		cryst
			A	A	x+1,y,z	0.0	664.7	544.7		cryst
P2Y1 receptor	4XNV	(Zhang, Gao, *et al.*, 2015)	A	A	y-x,-x,z	120.0	541.0	536.0		cryst
			A	A	-y,x-y,z	120.0	489.9	486.7		cryst
CXCR4 chemokine receptor	3OE8	(Wu *et al.*, 2010)	A	B	x+1,y,z	85.3	499.9	333.2		ncs
			B	A	x-1,y,z	85.3	492.2	236.7		ncs

A_{2A} adenosine receptor	4UG2	(Lebon *et al.*, 2015)	B	A	-x,y-1/2,1/2-z	84.2	455.8	319.6		ncs
			A	B	-x, 1/2+y, 1/2-z	84.2	413.2	197.9		ncs
CCR5 chemokine receptor	5NDD	(Cheng, Fiez-Vandal, *et al.*, 2017)	A	A	1+x,y,z	0.0	754.9	170.1		cryst
smoothened receptor	5V56	(Zhang, Zhao, *et al.*, 2017)	A	A	1+x,y,z	0.0	404.8	127.1		cryst
CCR5 chemokine receptor	5UIW	(Zheng *et al.*, 2017)	A	A	x-1,y,z	0.0	672.5	462.3		cryst
			A	A	1+x,y,z	0.0	676.5	586.2		cryst
glucagon receptor	5EE7	(Jazayeri *et al.*, 2016)	A	A	x-1,y,z	0.0	424.8	301.8		cryst
corticotropin-releasing factor receptor 1	4Z9G	(Dore *et al.*, 2017)	A	A	y,y-x,z	60.0	932.7	826.0		cryst
			A	A	x-y,x,z	60.0	976.6	924.6		cryst
corticotropin-releasing factor receptor 1	4Z9G	(Dore *et al.*, 2017)	B	C	x,y,z	59.7	1072.9	1016.2		ncs
			B	C	1-y,1+x-y,z	60.3	877.2	786.5		ncs
corticotropin-releasing factor receptor 1	4Z9G	(Dore *et al.*, 2017)	C	B	x,y,z	59.7	944.0	826.4		ncs
			C	B	y-x,1-x,z	60.4	992.3	890.0		ncs

Table 3 Interfaces between parallel GPCRs related by two-fold rotational symmetry. The central subunit is positioned as in the deposited PDB file. The symmetry operation is applied to the other chain's fractional coordinates. The rotation column is derived from the transformation relating the subunits' transmembrane helices. The buried solvent accessible surface (bSAS) values are for the central molecule and its transmembrane helices. Non-crystallographic (ncs) and crystallographic symmetry (cryst) are noted. Entries with no molecule name listed are the opposing faces for the interfaces listed immediately before them. The dimer label column is used throughout the rest of the paper to identify the dimers.

Molecule	PDB code	Reference	Central subunit	Second subunit	Symmetry operation	Rotation (°)	bSAS total	bSAS transmembrane helices	Symmetry	Dimer label
bovine opsin	4X1H	(Blankenship *et al.*, 2015)	A	A	-x,y-x,-z-1	180.0	832.6	785.0	cryst	1
CCR9 chemokine receptor	5LWE	(Oswald *et al.*, 2016)	A	B	x,y,z+1	176.7	621.7	292.0	ncs	2
			B	A	x,y,z-1	176.8	592.5	282.0	ncs	
μ-opioid receptor	4DKL	(Manglik *et al.*, 2012)	A	A	-x-1,y,-z-1	180.0	575.1	443.7	cryst	3
κ-opioid receptor	4DJH	(Wu *et al.*, 2012)	A	B	x,y,z	177.9	1003.9	687.0	ncs	4
			B	A	x,y,z	177.9	980.4	664.0	ncs	
β_1 adrenergic receptor	5F8U	(Leslie *et al.*, 2015)	B	A	x,y-1,z	179.3	798.9	376.1	ncs	5
			A	B	x,1+y,z	179.2	799.9	377.0	ncs	
β_1 adrenergic receptor	2VT4	(Warne *et al.*, 2008)	A	D	x-1,y,z+1	178.4	818.9	700.3	ncs	6
			D	A	x+1,y,z-1	178.3	812.4	701.5	ncs	
bovine rhodopsin	2I35	(Salom *et al.*, 2006)	A	A	2/3+x-y, 4/3-y,1/3-z	180.0	427.4	334.4	cryst	7
bovine rhodopsin	2I36	(Salom *et al.*, 2006)	C	C	x,x-y,1-z	180.0	666.0	459.5	cryst	8
bovine rhodopsin	2I36	(Salom *et*	B	A	x,y,z	176.6	495.6	365.2	ncs	9

		al., 2006)								
			A	B	x,y,z	176.6	485.2	377.9	ncs	
μ-opioid receptor	5C1M	(Huang *et al.*, 2015)	A	A	-x,-y+1/2,z	180.0	560.6	442.4	cryst	10
β_1 adrenergic receptor	2YCY	(Moukhametziano v *et al.*, 2011)	A	A	-x,y,-z	180.0	720.5	593.3	cryst	11
adenosine A_1 receptor	5N2S	(Cheng, Segala, *et al.*, 2017)	A	A	5/2-x,5/2-y,z	180.0	1397.5	426.0	cryst	12
metabotropic glutamate receptor 1	4OR2	(Wu *et al.*, 2014)	B	A	x,y,z	178.7	561.6	280.5	ncs	13
			A	B	x,y,z	178.7	508.6	289.1	ncs	
sphingosine 1-phosphate receptor	3V2Y	(Hanson *et al.*, 2012)	A	A	-x,1-y,z	180.0	773.3	277.7	cryst	14
CCR9 chemokine receptor	5LWE	(Oswald *et al.*, 2016)	A	B	x,y,z	176,8	495.1	495.1	ncs	15
			B	A	x,y,z	176.8	493.2	436.1	ncs	
smoothened receptor	4JKV	(Wang, Wu, *et al.*, 2013)	B	A	x,y,z	178.9	1203.2	1130.1	ncs	16
			A	B	x,y,z	179.0	1144.4	1026.1	ncs	
adenosine A_1 receptor	5N2S	(Cheng, Segala, *et al.*, 2017)	A	A	2-x,1-y,z	180.0	856.5	544.7	cryst	17
adenosine A_1 receptor	5UEN	(Glukhova *et al.*, 2017)	A	A	x,1-y,2-z	180.0	835.1	835.1	cryst	18
smoothened receptor	4QIN	(Wang *et al.*, 2014)	A	A	-x-1,y,-z	180.0	1268.7	1058.7	cryst	19
squid rhodopsin	2Z73	(Murakami & Kouyama, 2008)	B	B	1-x,1-y,z	180.0	516.3	417.7	cryst	20
CXCR4 chemokine receptor	3ODU	(Wu *et al.*, 2010)	B	A	x,y,z	179.8	921.2	692.8	ncs	21
			A	B	x,y,z	179.8	793.6	687.3	ncs	
CXCR4 chemokine receptor	4RWS	(Qin *et al.*, 2015)	A	A	2-x,-y,z	180.0	802.6	689.1	cryst	22

CXCR4 chemokine receptor	3OE6	(Wu *et al.*, 2010)	A	A	-x,1-y,z	180.0	754.1	612.3	cryst	23
CXCR4 chemokine receptor	3OE0	(Wu *et al.*, 2010)	A	A	1-x,y,-z	180.0	1047.5	954.0	cryst	24
β_1 adrenoceptor	4BVN		A	A	-x-1,y,-z	180.0	646.9	539.6	cryst	25
CXCR4 chemokine receptor	3OE8	(Wu *et al.*, 2010)	C	B	x,y,z	176.8	578.1	538.3	ncs	26
			B	C	x,y,z	176.8	576.9	530.2	ncs	
CXCR4 chemokine receptor	3OE9	(Wu *et al.*, 2010)	A	B	x,y,z	178.5	943.5	720.6	ncs	27
			B	A	x,y,z	178.6	863.3	570.8	ncs	
squid rhodopsin	2Z73	(Murakami & Kouyama, 2008)	A	A	1-x,1-y,z	180.0	620.2	397.1	cryst	28
squid rhodopsin	2ZIY	(Shimamura *et al.*, 2008)	A	A	x,-y,-z	180.0	690.1	430.0	cryst	29
μ-opioid receptor	4DKL	(Manglik *et al.*, 2012)	A	A	-x-1,y,-z	180.0	1452.1	1304.8	cryst	30
corticotropin-releasing factor receptor 1	4K5Y	(Hollenstein *et al.*, 2013)	C	C	x,-y,1-z	180.0	919.7	585.2	cryst	31

Table 4 Structural elements of the central molecule forming the dimer interface.

Dimer label (from Table 3)	TM1	TM2	TM3	TM4	TM5	TM6	TM7	H8
1	x	x				x	x	x
2	x							
3	x	x						x
4	x	x	x					x
5	x	x						x
6	x	x						
7	x	x						
8	x	x					x	x
9	x	x						
10	x	x						
11	x	x						
12	x	x						
13	x							
14			x	x				
15				x				
16			x	x	x			
17			x	x	x			
18			x	x	x			
19			x	x	x	x		
20				x	x			
21					x	x		
22			x	x	x			
23					x	x		
24			x	x	x	x		
25			x	x	x			
26					x	x		
27			x		x	x		
28			x		x			
29			x		x			
30					x	x		
31					x	x	x	

Table 5 Residues at the dimer interfaces. Generic GPCRdb numbering taken from http://gpcrdb.org/.

Dimer label (see Table 3)	1	2	3	4	5	6	7	8	9	10	11	12	13
Residue number	bovine opsin	CCR9 chemokine receptor	μ-opioid receptor	κ-opioid receptor	β_1 adrenergic receptor	β_1 adrenergic receptor	bovine rhodopsin	bovine rhodopsin	bovine rhodopsin	μ-opioid receptor	β_1 adrenergic receptor	adenosine A_1 receptor	metabotropic glutamate receptor 1
1x29				P56						M65			
1x32				P59	E41	E41							
1x33	S38			V60		A42				I69	A42		
1x34	M39												
1x35						M44							
1x36			M72	T63	S45	S45					S45		
1x37	A42	P53		A64	L46	L46					L46		
1x39				Y66									
1x40	F45	W56	S76	S67	A49	A49	F45		F45		A49		
1x41	L46	L57		V68		L50					L50		
1x43				F70		V52	I48				V52		
1x44		I60		V71	L53	L53	M49	M49	M49		L53	L1126	

1x47						V56		F52	F52		V56	V1129	
1x48								P53	P53			P1130	L605
1x51												V1133	L608
1x52												L1134	F609
1x55										Y91		W1137	L612
1x56													I613
1x59										R95			L616
1x60													Y617
2x55												A1165	
2x58				P113		P96					P96		
2x59				F114		F97							
2x61	L95			S116		A99					A99		
2x62			V126	T117		T100	Y96	Y96	Y96	V126	T100		
2x65	L99		L129	L120						L129			
2x66			M130		R104	R104		H100	H100	M130	R104		
3x20				F126									
6x32	E249												
6x35	R252												
7x43	T297												
7x47	V300												

7x48	Y301												
7x51	V304												
7x52	I305												
7x55								M308					
7x56	M309												
8x48									K311				
8x51				K338	R350			R314	R314				
8x54			F347	F341	F353								
8x55				R342	K354								
8x58			C351					L321					
8x59	C322		I352	F346				C322					

Acknowledgements I'm grateful to David Salom, Beata Jastrzebska, Philip Kiser, Isolde Le Trong, David Lodowski, Kris Palczewski, Peter Brzovic, and Dave Teller for encouragement and discussions of this and other GPCR-related topics.

References

Baltoumas, F. A., Theodorooulou, M. C. & Hamodrakas, S. J. (2016). *J. Comput. Aided Mol. Des.* **30**, 489-512.

Berman, H. M., Westbrook, J., Feng, Z., Gilliland, G., Bhat, T. N., Weissig, H., Shindyalov, I. N. & Bourne, P. E. (2000). *Nucleic Acids Res.* **28**, 235-242.

Blankenship, E., Vahedi-Faridi, A. & Lodowski, D. T. (2015). *Structure* **23**, 2358-2364.

Burg, J. S., Ingram, J. R., Venkatakrishnan, A. J., Jude, K. M., Dukkipati, A., Feinberg, E. N., Angelini, A., Waghray, D., Dror, R. O., Ploegh, H. L. & Garcia, K. C. (2015). *Science* **347**, 1113-1117.

Byrne, E. F. X., Sircar, R., Miller, P. S., Hedger, G., Luchetti, G., Nachtergaele, S., Tully, M. D., Mydock-McGrane, L., Covey, D. F., Rambo, R. P., Sansom, M. S. P., Newstead, S., Rohatgi, R. & Siebold, C. (2016). *Nature* **535**, 517-522.

Carpenter, B., Nehme, R., Warne, T., Leslie, A. G. W. & Tate, C. G. (2016). *Nature* **536**, 104-107.

Cheng, R. K. Y., Fiez-Vandal, C., Schlenker, O., Edman, K., Aggeler, B., Brown, D. G., Brown, G. A., Cooke, R. M., Dumelin, C. E., Dore, A. S., Geschwindner, S., Grebner, C., Hermansson, N.-O., Jazayeri, A., Johansson, P., Leong, L., Prihandoko, R., Rappas, M., Soutter, H., Snijder, A., Sundstrom, L., Tehan, B., Thornton, P., Troast, D., Wiggin, G., Zhukov, A., Marshall, F. H. & Dekker, N. (2017). *Nature* **545**, 112-115.

Cheng, R. K. Y., Segala, E., Robertson, N., Deflorian, F., Dore, A. S., Errey, J. C., Fiez-Vandal, C., Marshall, F. H. & Cooke, R. M. (2017). *Structure* **25**, 1275-1285.

Cherezov, V., Rosenbaum, D. M., Hanson, M. A., Rasmussen, S. G., Thian, F. S., Kobilka, T. S., Choi, H. J., Kuhn, P., Weis, W. I., Kobilka, B. K. & Stevens, R. C. (2007). *Science* **318**, 1258-1265.

Chien, E. Y., Liu, W., Zhao, Q., Katritch, V., Han, G. W., Hanson, M. A., Shi, L., Newman, A. H., Javitch, J. A., Cherezov, V. & Stevens, R. C. (2010). *Science* **330**, 1091-1095.

Chrencik, J. E., Roth, C. B., Terakado, M., Kurata, H., Omi, R., Kihara, Y., Warshaviak, D., Nakade, S., Asmar-Rovira, G., Mileni, M., Mizuno, H., Griffith, M. T., Rodgers, C., Han, G. W., Velasquez, J., Chun, J., Stevens, R. C. & Hanson, M. A. (2015). *Cell* **161**, 1633-1643.

Congreve, M., Andrews, S. P., Dore, A. S., Hollenstein, K., Hurrell, E., Langmead, C. J., Mason, J. S., Ng, I. W., Tehan, B., Zhukov, A., Weir, M. & Marshall, F. H. (2012). *J Med Chem* **55**, 1898-1903.

Dore, A. S., Bortolato, A., Hollenstein, K., Cheng, R. K. Y., Read, R. J. & Marshall, F. H. (2017). *Current Molecular Pharmacology* **10**, 334-344.

Dore, A. S., Okrasa, K., Patel, J. C., Serrano-Vega, M., Bennett, K., Cooke, R. M., Errey, J. C., Jazayeri, A., Khan, S., Tehan, B., Weir, M., Wiggin, G. R. & Marshall, F. H. (2014). *Nature* **511**, 557-562.

Duarte, J. M., Biyani, N., Baskaran, K. & Capitani, G. (2013). *Bmc Structural Biology* **13**.

Duarte, J. M., Srebniak, A., Scharer, M. A. & Capitani, G. (2012). *BMC Bioinformatics* **13**, 334.

Egloff, P., Hillenbrand, M., Klenk, C., Batyuk, A., Heine, P., Balada, S., Schlinkmann, K. M., Scott, D. J., Schutz, M. & Pluckthun, A. (2014). *Proc Natl Acad Sci U S A* **111**, E655-662.

Emsley, P., Lohkamp, B., Scott, W. G. & Cowtan, K. (2010). *Acta Cryst.* **D66**, 486-501.

Farran, B. (2017). *Pharmacological Research* **117**, 303-327.

Fenalti, G., Giguere, P. M., Katritch, V., Huang, X. P., Thompson, A. A., Cherezov, V., Roth, B. L. & Stevens, R. C. (2014). *Nature* **506**, 191-196.

Fenalti, G., Zatsepin, N. A., Betti, C., Giguere, P., Han, G. W., Ishchenko, A., Liu, W., Guillemyn, K., Zhang, H., James, D., Wang, D., Weierstall, U., Spence, J. C., Boutet, S., Messerschmidt, M., Williams, G. J., Gati, C., Yefanov, O. M., White, T. A., Oberthuer, D., Metz, M., Yoon, C. H., Barty, A., Chapman, H. N., Basu, S., Coe, J., Conrad, C. E., Fromme, R., Fromme, P., Tourwe, D., Schiller, P. W., Roth, B. L., Ballet, S., Katritch, V., Stevens, R. C. & Cherezov, V. (2015). *Nat Struct Mol Biol* **22**, 265-268.

Ferre, S., Casado, V., Devi, L. A., Filizola, M., Jockers, R., Lohse, M. J., Milligan, G., Pin, J. P. & Guitart, X. (2014). *Pharmacol. Rev.* **66**, 413-434.

Filipek, S., Krzysko, K. A., Fotiadis, D., Liang, Y., Saperstein, D. A., Engel, A. & Palczewski, K. (2004). *Photochem Photobiol Sci* **3**, 628-638.

Fotiadis, D., Liang, Y., Filipek, S., Saperstein, D. A., Engel, A. & Palczewski, K. (2003). *Nature* **421**, 127-128.

Gahbauer, S. & Böckmann, R. A. (2016). *Frontiers in Physiology* **7**, Article 494.

Glukhova, A., Thal, D. M., Nguyen, A. T., Vecchio, E. A., Jorg, M., Scammells, P. J., May, L. T., Sexton, P. M. & Christopoulos, A. (2017). *Cell* **168**, 867-877.

Granier, S., Manglik, A., Kruse, A. C., Kobilka, T. S., Thian, F. S., Weis, W. I. & Kobilka, B. K. (2012). *Nature* **485**, 400-404.

Gulati, S., Jastrzebska, B., Banerjee, S., Placeres, A. L., Miszta, P. G., S., Gunderson, K., Tochtrop, G. P., Filipek, S., Katayama, K., Kiser, P. D., Mogi, M., Stewart, P. L. & Palczewski, K. (2017). *Proc. Natl. Acad. Sci. U. S. A.* **114**, E2608-E2615.

Haga, K., Kruse, A. C., Asada, H., Yurugi-Kobayashi, T., Shiroishi, M., Zhang, C., Weis, W. I., Okada, T., Kobilka, B. K., Haga, T. & Kobayashi, T. (2012). *Nature* **482**, 547-551.

Hanson, M. A., Roth, C. B., Jo, E., Griffith, M. T., Scott, F. L., Reinhart, G., Desale, H., Clemons, B., Cahalan, S. M., Schuerer, S. C., Sanna, M. G., Han, G. W., Kuhn, P., Rosen, H. & Stevens, R. C. (2012). *Science* **335**, 851-855.

Hino, T., Arakawa, T., Iwanari, H., Yurugi-Kobayashi, T., Ikeda-Suno, C., Nakada-Nakura, Y., Kusano-Arai, O., Weyand, S., Shimamura, T., Nomura, N., Cameron, A. D., Kobayashi, T., Hamakubo, T., Iwata, S. & Murata, T. (2012). *Nature* **482**, 237-240.

Hollenstein, K., Kean, J., Bortolato, A., Cheng, R. K., Dore, A. S., Jazayeri, A., Cooke, R. M., Weir, M. & Marshall, F. H. (2013). *Nature* **499**, 438-443.

Hua, T., Vemuri, K., Nikas, S. P., Laprairie, R. B., Wu, Y., Qu, L., Pu, M., Korde, A., Jiang, S., Ho, J.-H., Han, G. W., Ding, K., Li, X., Liu, H., Hanson, M. A., Zhao, S., Bohn, L. M., Makriyannis, A., Stevens, R. C. & Liu, Z.-J. (2017). *Nature* **547**, 468-471.

Hua, T., Vemuri, K., Pu, M., Qu, L., Han, G. W., Wu, Y., Zhao, S., Shui, W., Li, S., Korde, A., Laprairie, R. B., Stahl, E. L., Ho, J.-H., Zvonok, N., Zhou, H., Kufareva, I., Wu, B., Zhao, Q., Hanson, M. A., Bohn, L. M., Makriyannis, A., Stevens, R. C. & Liu, Z.-J. (2016). *Cell* **167**, 750-762.

Huang, J. Y., Chen, S., Zhang, J. J. & Huang, X. Y. (2013). *Nature Structural & Molecular Biology* **20**, 419-425.

Huang, W., Manglik, A., Venkatakrishnan, A. J., Laeremans, T., Feinberg, E. N., Sanborn, A. L., Kato, H. E., Livingston, K. E., Thorsen, T. S., Kling, R. C., Granier, S., Gmeiner, P., Husbands, S. M., Traynor, J. R., Weis, W. I., Steyaert, J., Dror, R. O. & Kobilka, B. K. (2015). *Nature* **524**, 315-321.

Isberg, V., Mordalski, S., Munk, C., Rataj, K., Harpsøe, K., Hauser, A. S., Vroling, B., Bojarski, A. J., Vriend, G. & Gloriam, D. E. (2016). *Nucl. Acids. Res.* **44**, D356-D364.

Ishchenko, A., Wacker, D., Kapoor, M., Zhang, A., Han, G. W., Basu, S., Patel, N., Messerschmidt, M., Weierstall, U., Liu, W., Katritch, V., Roth, B. L., Stevens, R. C. & Cherezov, V. (2017). *Proc Natl Acad Sci U S A* **114**, 8223-8228.

Jaakola, V. P., Griffith, M. T., Hanson, M. A., Cherezov, V., Chien, E. Y., Lane, J. R., Ijzerman, A. P. & Stevens, R. C. (2008). *Science* **322**, 1211-1217.

Janin, J. (1997). *Nat. Struct. Biol.* **4**, 973-974.

Jastrzebska, B., Comar, W. D., Kaliszewski, M. J., Skinner, K. C., Torcasio, M. H., Esway, A. S., Jin, H., Palczewski, K. & Smith, A. W. (2016). *Biochemistry* **56**, 61-72.

Jastrzebska, B., Ringler, P., Lodowski, D. T., Molseenkova-Bell, V., Golczak, M., Müller, S. A., Palczewski, K. & Engel, A. (2011). *J. Struct. Biol* **176**, 387-394.

Jastrzebska, B., Ringler, P., Palczewski, K. & Engel, A. (2013). *J. Struct. Biol.* **182**, 164-172.

Jazayeri, A., Dore, A. S., Krishnamurthy, H., Southall, S. M., Haig, A. S., Bortolato, A., Koglin, M., Robertson, N. J., Errey, J. C., Andrews, S. P., Teobald, I., Brown, A. J. H., Cooke, R. M., Weir, M. & Marshall, F. H. (2016). *Nature* **533**, 274-277.

Jazayeri, A., Rappas, M., Brown, A. J. H., Kean, J., Errey, J. C., Robertson, N. J., Fiez-Vandal, C., Andrews, S. P., Congreve, M., Bortolato, A., Mason, J. S., Baig, A. H., Teobald, I., Dore, A. S., Weir, M., Cooke, R. M. & Marshall, F. H. (2017). *Nature* **546**, 254-258.

Kasai, R. S. & Kusumi, A. (2014). *Curr. Opin. Cell Biol.* **27**, 78-86.

Katritch, V., Cherezov, V. & Stevens, R. C. (2013). *Annu. Rev. Pharmacol. Toxicol.* **53**, 531-556.

Kraulis, P. J. (1991). *J. Appl. Crystallogr.* **24**, 946-950.

Krissinel, E. & Henrick, K. (2004). *Acta Cryst.* **D60**, 2256-2268.

Krumm, B. E., Lee, S., Bhattacharya, S., Botos, I., White, C. F., Du, H., Vaidehi, N. & Grisshammer, R. (2016). *Scientific Reports* **6**, 38564

Krumm, B. E., White, J. F., Shah, P. & Grisshammer, R. (2015). *Nat Commun* **6**, 7895.

Kruse, A. C., Hu, J., Pan, A. C., Arlow, D. H., Rosenbaum, D. M., Rosemond, E., Green, H. F., Liu, T., Chae, P. S., Dror, R. O., Shaw, D. E., Weis, W. I., Wess, J. & Kobilka, B. K. (2012). *Nature* **482**, 552-556.

Lebon, G., Edwards, P. C., Leslie, A. G. & Tate, C. G. (2015). *Mol Pharmacol* **87**, 907-915.

Lebon, G., Warne, T., Edwards, P. C., Bennett, K., Langmead, C. J., Leslie, A. G. & Tate, C. G. (2011). *Nature* **474**, 521-525.

Lee, B. & Richards, F. M. (1971). *J. Mol. Biol.* **55**, 379-400.

Leslie, A. G. W., Warne, T. & Tate, C. G. (2015). *Nature Structural & Molecular Biology* **22**, 941-942.

Liang, Y., Fotiadis, D., Filipek, S., Saperstein, D. A., Palczewski, K. & Engel, A. (2003). *J Biol Chem* **278**, 21655-21662.

Liu, X., Ahn, S., Kahsai, A. W., Meng, K.-C., Latorraca, N. R., Pani, B., Venkatakrishnan, A. J., Masoudi, A., Weis, W. I., Dror, R. O., Chen, X., Lefkowitz, R. J. & Kobilka, B. (2017). *Nature* **548**, 480-484.

Lu, J., Byrne, N., Wang, J., Bricogne, G., Brown, F. K., Chobanian, H. R., Colletti, S. I., Di Salvo, J., Thomas-Fowlkes, B., Guo, Y., Hall, D. L., Hadix, J., Hastings, N. B., Hermes, J. D., Ho, T., Howard, A. D., Josien, H., Kornienko, M., Lumb, K. J., Miller, M. W., Patel, S. B., Pio, B., Plummer, C. W., Sherborne, B. S., Sheth, P., Souza, S., Tummala, S., Vonrhein, C., Webb, M., Allen, S. J., Johnston, J. M., Weinglass, A. B., Sharma, S. & Soisson, S. M. (2017). *Nature Structural & Molecular Biology* **24**, 570-577.

Ma, Y., Yue, Y., Ma, Y., Zhang, Q., Zhou, Q., Song, Y., Shen, Y., Li, X., Ma, X., Li, C., Hanson, M. A., Han, G. W., Sickmier, E. A., Swaminath, G., Zhao, S., Stevens, R. C., Hu, L. A., Zhong, W., Zhang, M. & Xu, F. (2017). *Structure* **25**, 858-866.

Manglik, A., Kruse, A. C., Kobilka, T. S., Thian, F. S., Mathiesen, J. M., Sunahara, R. K., Pardo, L., Weis, W. I., Kobilka, B. K. & Granier, S. (2012). *Nature* **485**, 321-326.

McRee, D. E. (1999). *J. Structural Biology*. **125**, 156-165.

Merritt, E. A. & Bacon, D. J. (1997). *Meth. Enzym.* **277**, 505-524.

Miller-Gallacher, J. L., Nehme, R., Warne, T., Edwards, P. C., Schertler, G. F., Leslie, A. G. & Tate, C. G. (2014). *PLOS One* **9**, e92727.

Miller, R. L., Thompson, A. A., Trapella, C., Guerrini, R., Malfacini, D., Patel, N., Han, G. W., Cherezov, V., Calo, G., Katritch, V. & Stevens, R. C. (2015). *Structure* **23**, 2291-2299.

Moukhametzianov, R., Warne, T., Edwards, P. C., Serrano-Vega, M. J., Leslie, A. G., Tate, C. G. & Schertler, G. F. (2011). *Proc Natl Acad Sci U S A* **108**, 8228-8232.

Murakami, M. & Kouyama, T. (2008). *Nature* **453**, 363-367.

Okada, T. (2012). *PLoS ONE* **7**, e35802.

Okada, T., Sugihara, M., Bondar, A.-N., Elstner, M., Entel, P. & Buss, V. (2004). *J. Mol. Biol.* **343**, 571-583.

Oswald, C., Rappas, M., Kean, J., Dore, A. S., Errey, J. C., Bennett, K., Deflorian, F., Christopher, J. A., Jazayeri, A., Mason, J. S., Congreve, M., Cooke, R. M. & Marshall, F. H. (2016). *Nature* **540**, 462-465.

Palczewski, K., Kumasaka, T., Hori, T., Behnke, C. A., Motoshima, H., Fox, B. A., Le Trong, I., Teller, D. C., Okada, T., Stenkamp, R. E., Yamamoto, M. & Miyano, M. (2000). *Science* **289**, 739-745.

Palczewski, K. & Orban, T. (2013). *Annu. Rev. Neurosci.* **36**, 139-164.

Piscitelli, C. L., Kean, J., de Graaf, C. & Deupi, X. (2015). *Mol. Pharmacol.* **88**, 536-551.

Qin, L., Kufareva, I., Holden, L. G., Wang, C., Zheng, Y., Zhao, C., Fenalti, G., Wu, H., Han, G. W., Cherezov, V., Abagyan, R., Stevens, R. C. & Handel, T. M. (2015). *Science* **347**, 1117-1122.

Rasmussen, S. G., Choi, H. J., Fung, J. J., Pardon, E., Casarosa, P., Chae, P. S., Devree, B. T., Rosenbaum, D. M., Thian, F. S., Kobilka, T. S., Schnapp, A., Konetzki, I., Sunahara, R. K., Gellman, S. H., Pautsch, A., Steyaert, J., Weis, W. I. & Kobilka, B. K. (2011). *Nature* **469**, 175-180.

Rasmussen, S. G., Choi, H. J., Rosenbaum, D. M., Kobilka, T. S., Thian, F. S., Edwards, P. C., Burghammer, M., Ratnala, V. R., Sanishvili, R., Fischetti, R. F., Schertler, G. F., Weis, W. I. & Kobilka, B. K. (2007). *Nature* **450**, 383-387.

Rasmussen, S. G., DeVree, B. T., Zou, Y., Kruse, A. C., Chung, K. Y., Kobilka, T. S., Thian, F. S., Chae, P. S., Pardon, E., Calinski, D., Mathiesen, J. M., Shah, S. T., Lyons, J. A., Caffrey, M., Gellman, S. H., Steyaert, J., Skiniotis, G., Weis, W. I., Sunahara, R. K. & Kobilka, B. K. (2011). *Nature* **477**, 549-555.

Ring, A. M., Manglik, A., Kruse, A. C., Enos, M. D., Weis, W. I., Garcia, K. C. & Kobilka, B. K. (2013). *Nature* **502**, 575-579.

Rosenbaum, D. M., Zhang, C., Lyons, J. A., Holl, R., Aragao, D., Arlow, D. H., Rasmussen, S. G., Choi, H. J., Devree, B. T., Sunahara, R. K., Chae, P. S., Gellman, S. H., Dror, R. O., Shaw, D. E., Weis, W. I., Caffrey, M., Gmeiner, P. & Kobilka, B. K. (2011). *Nature* **469**, 236-240.

Saff, E. B. & Kuijlaars, A. B. J. (1997). *The Mathematical Intelligencer* **19**, 5-11.

Salom, D., Lodowski, D. T., Stenkamp, R. E., Le Trong, I., Golczak, M., Jastrzebska, B., Harris, T., Ballesteros, J. A. & Palczewski, K. (2006). *Proc. Natl. Acad. Sci. U.S.A.* **103**, 16123-16128.

Sato, T., Kawasaki, T., Mine, S. & Matsumura, H. (2016). *Int. J. Mol. Sci.* **17**, ijms17111930.

Shao, Z., Yin, J., Chapman, K., Grzemska, M., Clark, L., Wang, J. & Rosenbaum, D. M. (2016). *Nature* **540**, 602-606.

Shihoya, W., Nishizawa, T., Okuta, A., Tani, K., Dohmae, N., Fujiyoshi, Y., Nureki, O. & Doi, T. (2016). *Nature* **537**, 363-368.

Shihoya, W., Nishizawa, T., Yamashita, K., Inoue, A., Hirata, K., Kadji, F. M. N., Okuta, A., Tani, K., Aoki, J., Fujiyoshi, Y., Doi, T. & Nureki, O. (2017). *Nature Structural & Molecular Biology* **24**, 758-764.

Shimamura, T., Hiraki, K., Takahashi, N., Hori, T., Ago, H., Masuda, K., Takio, K., Ishiguro, M. & Miyano, M. (2008). *J Biol Chem* **283**, 17753-17756.

Shimamura, T., Shiroishi, M., Weyand, S., Tsujimoto, H., Winter, G., Katritch, V., Abagyan, R., Cherezov, V., Liu, W., Han, G. W., Kobayashi, T., Stevens, R. C. & Iwata, S. (2011). *Nature* **475**, 65-70.

Siu, F. Y., He, M., de Graaf, C., Han, G. W., Yang, D., Zhang, Z., Zhou, C., Xu, Q., Wacker, D., Joseph, J. S., Liu, W., Lau, J., Cherezov, V., Katritch, V., Wang, M. W. & Stevens, R. C. (2013). *Nature* **499**, 444-449.

Song, G., Yang, D., Wang, Y., De Graff, C., Q., Z., Jiang, S., Liu, K., Cai, X., Dai, A., Lin, G., Liu, D., Wu, F., Wu, Y., Zhao, S., Ye, L., Han, G. W., Lau, J., Wu, B., Hanson, M. A., Liu, Z.-J., Wang, M.-W. & Stevens, R. C. (2017). *Nature* **546**, 312-315.

Staus, D. P., Strachan, R. T., Manglik, A., Pani, B., Kahsai, A. W., Kim, T. H., Wingler, L. M., Ahn, S., Chatterjee, A., Masoudi, A., Kruse, A. C., Pardon, E., Steyaert, J., Weis, W. I., Prosser, R. S., Kobilka, B. K., Costa, T. & Lefkowitz, R. J. (2016). *Nature* **535**, 448-452.

Stenkamp, R. E. (2008). *Acta Crystallogr D Biol Crystallogr* **D64**, 902-904.

Sun, B., Bachhawat, P., Chu, M. L.-H., Wood, M., Ceska, T., Sands, Z. A., Mercier, J., Lebon, F., Kobilka, T. S. & Kobilka, B. K. (2017). *Proc Natl Acad Sci U S A* **114**, 2066-2071.

Tan, Q., Zhu, Y., Li, J., Chen, Z., Han, G. W., Kufareva, I., Li, T., Ma, L., Fenalti, G., Zhang, W., Xie, X., Yang, H., Jiang, H., Cherezov, V., Liu, H., Stevens, R. C., Zhao, Q. & Wu, B. (2013). *Science* **341**, 1387-1390.

Taniguchi, R., Inoue, A., Sayama, M., Uwamizu, A., Yamashita, K., Hirata, K., Yoshida, M., Tanaka, Y., Kato, H. E., Nakada-Nakura, Y., Otani, Y., Nishizawa, T., Doi, T., Ohwada, T., Ishitani, R., Aoki, J. & Nureki, O. (2017). *Nature* **548**, 356-360.

Thal, D. M., Sun, B., Feng, D., Nawaratne, V., Leach, K., Felder, C. C., Bures, M. G., Evans, D. A., Weis, W. I., Bachhawat, P., Kobilka, T. S., Sexton, P. M., Kobilka, B. K. & Christopoulos, A. (2016). *Nature* **531**, 335-340.

Thorsen, T. S., Matt, R., Weis, W. I. & Kobilka, B. K. (2014). *Structure* **22**, 1657-1664.

Tian, H., Fürstenberg, A. & Huber, T. (2017). *Chem. Rev.* **117**, 186-245.

Vischer, H. F., Castro, M. & Pin, J. P. (2015). *Mol. Pharmacol.* **88**, 561-571.

Wacker, D., Wang, C., Katritch, V., Han, G. W., Huang, X. P., Vardy, E., McCorvy, J. D., Jiang, Y., Chu, M., Siu, F. Y., Liu, W., Xu, H. E., Cherezov, V., Roth, B. L. & Stevens, R. C. (2013). *Science* **340**, 615-619.

Wang, C., Jiang, Y., Ma, J., Wu, H., Wacker, D., Katritch, V., Han, G. W., Liu, W., Huang, X. P., Vardy, E., McCorvy, J. D., Gao, X., Zhou, X. E., Melcher, K., Zhang, C., Bai, F., Yang, H., Yang, L., Jiang, H., Roth, B. L., Cherezov, V., Stevens, R. C. & Xu, H. E. (2013). *Science* **340**, 610-614.

Wang, C., Wu, H., Evron, T., Vardy, E., Han, G. W., Huang, X. P., Hufeisen, S. J., Mangano, T. J., Urban, D. J., Katritch, V., Cherezov, V., Caron, M. G., Roth, B. L. & Stevens, R. C. (2014). *Nat Commun* **5**, 4355.

Wang, C., Wu, H., Katritch, V., Han, G. W., Huang, X. P., Liu, W., Siu, F. Y., Roth, B. L., Cherezov, V. & Stevens, R. C. (2013). *Nature* **497**, 338-343.

Wang, S., Wacker, D., Levit, A., Che, T., Betz, R. M., McCorvy, J. D., Venkatakrishnan, A. J., Huang, X.-P., Dror, R. O., Shoichet, B. K. & Roth, B. L. (2017). *Science* **358**, 381-386.

Warne, T., Edwards, P. C., Leslie, A. G. & Tate, C. G. (2012). *Structure* **20**, 841-849.

Warne, T., Serrano-Vega, M. J., Baker, J. G., Moukhametzianov, R., Edwards, P. C., Henderson, R., Leslie, A. G., Tate, C. G. & Schertler, G. F. (2008). *Nature* **454**, 486-491.

Weierstall, U., James, D., Wang, C., White, T. A., Wang, D., Liu, W., Spence, J. C., Bruce Doak, R., Nelson, G., Fromme, P., Fromme, R., Grotjohann, I., Kupitz, C., Zatsepin, N. A., Liu, H., Basu, S., Wacker, D., Han, G. W., Katritch, V., Boutet, S., Messerschmidt, M., Williams, G. J., Koglin, J. E., Marvin Seibert, M., Klinker, M., Gati, C., Shoeman, R. L., Barty, A., Chapman, H. N., Kirian, R. A., Beyerlein, K. R., Stevens, R. C., Li, D., Shah, S. T., Howe, N., Caffrey, M. & Cherezov, V. (2014). *Nat Commun* **5**, 3309.

Weinert, T., Olieric, N., Cheng, R. K., Brunle, S., James, D., Ozerov, D., Gashi, D., Vera, L., Marsh, M., Jaeger, K., Dworkowski, F. S. N., Panepucci, E., Basu, S., Skopintsev, P., Dore, A. S., Geng, T., Cooke, R. M., Liang, M., Prota, A. E., Panneels, V., Nogly, P., Ermler, U., Schertler, G., Hennig, M., Steinmetz, M. O., Wang, M. & Standfuss, J. (2017). *Nature Communications*.

White, J. F., Noinaj, N., Shibata, Y., Love, J., Kloss, B., Xu, F., Gvozdenovic-Jeremic, J., Shah, P., Shiloach, J., Tate, C. G. & Grisshammer, R. (2012). *Nature* **490**, 508-513.

Winn, M. D., Ballard, C. C., Cowtan, K. D., Dodson, E. J., Emsley, P., Evans, P. R., Keegan, R. M., Krissinel, E. B., Leslie, A. G. W., McCoy, A., McNicholas, S. J., Murshudov, G. N., Pannu, N. S., Potterton, E. A., Powell, H. R., Read, R. J., Vagin, A. & Wilson, K. S. (2011). *Acta Cryst.* **D67**, 235-242.

Wu, B., Chien, E. Y., Mol, C. D., Fenalti, G., Liu, W., Katritch, V., Abagyan, R., Brooun, A., Wells, P., Bi, F. C., Hamel, D. J., Kuhn, P., Handel, T. M., Cherezov, V. & Stevens, R. C. (2010). *Science* **330**, 1066-1071.

Wu, H., Wacker, D., Mileni, M., Katritch, V., Han, G. W., Vardy, E., Liu, W., Thompson, A. A., Huang, X. P., Carroll, F. I., Mascarella, S. W., Westkaemper, R. B., Mosier, P. D., Roth, B. L., Cherezov, V. & Stevens, R. C. (2012). *Nature* **485**, 327-332.

Wu, H., Wang, C., Gregory, K. J., Han, G. W., Cho, H. P., Xia, Y., Niswender, C. M., Katritch, V., Meiler, J., Cherezov, V., Conn, P. J. & Stevens, R. C. (2014). *Science* **344**, 58-64.

Yin, J., Babaoglu, K., Brautigam, C. A., Clark, L., Shao, Z., Scheuermann, T. H., Harrell, C. M., Gotter, A. L., Roecker, A. J., Winrow, C. J., Renger, J. J., Coleman, P. J. & Rosenbaum, D. M. (2016). *Nat Struct Mol Biol* **23**, 293-299.

Yin, J., Mobarec, J. C., Kolb, P. & Rosenbaum, D. M. (2015). *Nature* **519**, 247-250.

Zhang, C., Srinivasan, Y., Arlow, D. H., Fung, J. J., Palmer, D., Zheng, Y., Green, H. F., Pandey, A., Dror, R. O., Shaw, D. E., Weis, W. I., Coughlin, S. R. & Kobilka, B. K. (2012). *Nature* **492**, 387-392.

Zhang, D., Gao, Z. G., Zhang, K., Kiselev, E., Crane, S., Wang, J., Paoletta, S., Yi, C., Ma, L., Zhang, W., Han, G. W., Liu, H., Cherezov, V., Katritch, V., Jiang, H., Stevens, R. C., Jacobson, K. A., Zhao, Q. & Wu, B. (2015). *Nature* **520**, 317-321.

Zhang, H., Han, G. W., Batyuk, A., Ishchenko, A., While, K. L., Patel, N., Sadybekov, A., Zamlynny, B., Rudd, M. T., Hollenstein, K., Tolstikova, A., White, T. A., Hunter, M. S., Weierstall, U., Liu, W., Babaoglu, K., Moore, E. L., Katz, R. D., Shipman, J. M., Garcia-Calvo, M., Sharma, S., Sheth, P., Soisson, S. M., Stevens, R. C., Katritch, V. & Cherezov, V. (2017). *Nature* **544**, 327-332.

Zhang, H., Qiao, A., Yang, D., Yang, L., Dai, A., De Graaf, C., Reedtz-Runge, S., Dharmarajan, V., Zhang, H., Han, G. W., Grant, T. D., Sierra, R. G., Weierstall, U., Nelson, G., Liu, W., Wu, Y., Ma, L., Cai, X., Lin, G., Wu, X., Geng, Z., Dong, Y., Song, G., Griffin, P. R., Lau, J., Cherezov, V., Yang, H., Hanson, M. A., Stevens, R. C., Zhao, Q., Jiang, H., Wang, M.-W. & Wu, B. (2017). *Nature* **546**, 259-264.

Zhang, H., Unal, H., Desnoyer, R., Han, G. W., Patel, N., Katritch, V., Karnik, S. S., Cherezov, V. & Stevens, R. C. (2015). *J Biol Chem* **290**, 29127-29139.

Zhang, H., Unal, H., Gati, C., Han, G. W., Liu, W., Zatsepin, N. A., James, D., Wang, D., Nelson, G., Weierstall, U., Sawaya, M. R., Xu, Q., Messerschmidt, M., Williams, G. J., Boutet, S., Yefanov, O. M., White, T. A., Wang, C., Ishchenko, A., Tirupula, K. C., Desnoyer, R., Coe, J., Conrad, C. E., Fromme, P., Stevens, R. C., Katritch, V., Karnik, S. S. & Cherezov, V. (2015). *Cell* **161**, 833-844.

Zhang, J., Zhang, K., Gao, Z. G., Paoletta, S., Zhang, D., Han, G. W., Li, T., Ma, L., Zhang, W., Muller, C. E., Yang, H., Jiang, H., Cherezov, V., Katritch, V., Jacobson, K. A., Stevens, R. C., Wu, B. & Zhao, Q. (2014). *Nature* **509**, 119-122.

Zhang, K., Zhang, J., Gao, Z. G., Zhang, D., Zhu, L., Han, G. W., Moss, S. M., Paoletta, S., Kiselev, E., Lu, W., Fenalti, G., Zhang, W., Muller, C. E., Yang, H., Jiang, H., Cherezov, V., Katritch, V., Jacobson, K. A., Stevens, R. C., Wu, B. & Zhao, Q. (2014). *Nature* **509**, 115-118.

Zhang, X., Zhao, F., Wu, Y., Yang, J., Han, G. W., Zhao, S., Ishchenko, A., Ye, L., Lin, X., Ding, K., Dharmarajan, V., Griffin, P. R., Gati, C., Nelson, G., Hunter, M. S., Hanson, M. A., Cherezov, V., Stevens, R. C., Tan, W., Tao, H. & Xu, F. (2017). *Nature Communications* **8**, 15383.

Zheng, Y., Han, G. W., Abagyan, R., Wu, B., Stevens, R. C., Cherezov, V., Kufareva, I. & Handel, T. M. (2017). *Immunity* **46**, 1005-1017.

Zheng, Y., Qin, L., Ortiz Zacarias, N. V., de Vries, H., Han, G. W., Gustavsson, M., Dabros, M., Zhao, C., Cherney, R. J., Carter, P., Stamos, D., Abagyan, R., Cherezov, V., Stevens, R. C., Uzerman, A. P., Heitman, L. H., Tebben, A., Kufareva, I. & Handel, T. M. (2016). *Nature* **540**, 458-461.

Zhou, X. E., He, Y., De Waal, P. W., Gao, X., Kang, Y., Van Eps, N., Yin, Y., Pal, K., Goswami, D., White, T. A., Barty, A., Latorraca, N. R., Chapman, H. N., Hubbell, W. L., Dror, R. O., Stevens, R. C., Cherezov, V., Gurevich, V. V., Griffin, P. R., Ernst, O. P., Melcher, K. & Xu, H. E. (2017). *Cell* **170**, 457-469.

Zou, Y., Weis, W. I. & Kobilka, B. K. (2012). *PLOS One* **7**, e46039.